

## Submarine topography-related spatial variability of the southern Taiwan Strait sands (East Asia)

Xiaotian Shen<sup>a</sup>, Xing Jian<sup>a,\*</sup>, Chao Li<sup>a</sup>, James T. Liu<sup>b</sup>, Yuan-Pin Chang<sup>b</sup>, Shuo Zhang<sup>c</sup>, Haowei Mei<sup>a</sup>, Hanjing Fu<sup>a</sup>, Wei Zhang<sup>a</sup>

<sup>a</sup> State Key Laboratory of Marine Environmental Science, College of Ocean and Earth Sciences, Xiamen University, Xiamen 361102, PR China

<sup>b</sup> Department of Oceanography, National Sun Yat-sen University, Kaohsiung 80424, Taiwan

<sup>c</sup> Collaborative Innovation Center of South China Sea Studies, Nanjing University, Nanjing, Jiangsu Province 210023, PR China

### ARTICLE INFO

#### Keywords:

Taiwan Strait  
Provenance analysis  
Petrography  
Heavy mineral analysis  
Sediment source-to-sink  
East Asia continental margin

### ABSTRACT

The Taiwan Strait serves as a link between the East China Sea and South China Sea in East Asia. Complex ocean dynamics, huge sediment inputs and distinct tectonic, climatic and bedrock lithological settings of the two sides of the strait make it ideal for sediment source-to-sink studying. While mud sediments in the strait have been well investigated, sand composition and provenance remain understudied. Here, we present framework petrography and heavy mineral data of sands from the southern Taiwan Strait and the adjacent representative rivers to characterize sand provenance and depositional mechanisms. As expected, the SE China river sands are dominated by quartz and feldspar, whereas sands from the westward-flowing mountainous rivers in Taiwan are rich in lithic fragments and heavy minerals of metamorphic origin. The southern Taiwan Strait sands show significant spatial variations in composition and texture of the framework grains and heavy minerals. Framework grain-based provenance modeling results show that sands in the southwest margin of Taiwan Strait (water depth of 30–60 m) are mainly supplied by SE China rivers. Taiwan mountainous rivers made prominent contributions to the central-western Taiwan Strait (40–60 m) and the south of Taiwan Shoal (below 50 m), both of which are far away from the Taiwan island (ca. 100–300 km away). Furthermore, sands from the Taiwan Shoal (20–30 m) show extremely high compositional maturity and are mainly composed of coarse, rounded quartz. These sands, previously proposed as relict sediments, have been intensely altered by modern high-energy hydrodynamic conditions and can also be interpreted as palimpsest sediments. These results demonstrate that modern river-derived sands are eventually deposited in relatively deep-water regions in the strait, rather than the shallow regions (Taiwan Shoal). We propose that the sand composition and distribution are closely related to the submarine topography of the Taiwan Strait. Combining previous mud belt investigations, we suggest that sands and muds tend to have different fates in shallow continental shelves with complex climate, ocean current and seafloor landform conditions. This study also highlights the importance of both modern and relict sands in the strait and our findings are important to better understanding of shelf sedimentary systems with huge river-sediment-input and high wave/tidal-current-energy.

### 1. Introduction

Continental shelves locate in regions between continents and open oceans and provide pathways for sediment transport from land to the deep ocean, and thus play an important role in global sediment source-to-sink systems (Kao and Milliman, 2008; Yang et al., 2014b; Liu et al., 2016). Generally, global continental shelves are characterized by flat topography with water depth above 200 m, but show remarkable

diversity over horizontal scales. For example, the western coast of South America and southern coast of the Philippines are less than 10 km in width, whereas the Barents Sea shelf and the East China Sea (ECS) shelf are broader than 500 km. Broad continental shelves also commonly serve as an important sink for terrestrial sediments (Nittrouer and Demaster, 1986; Thomas et al., 2004; Liu et al., 2006, 2007; Xu et al., 2012; Wang et al., 2013; Bi et al., 2015, 2017; Deng et al., 2017, 2019) and sedimentary successions therein can preserve essential information

\* Corresponding author.

E-mail address: [xjian@xmu.edu.cn](mailto:xjian@xmu.edu.cn) (X. Jian).

<https://doi.org/10.1016/j.margeo.2021.106495>

Received 9 December 2020; Received in revised form 24 March 2021; Accepted 20 April 2021

Available online 24 April 2021

0025-3227/© 2021 Elsevier B.V. All rights reserved.

concerning sea level change, climatic evolution and land-ocean interactions over different timescales (Wang, 1999; Eiriksson et al., 2000; Rasmussen et al., 2007; Yang et al., 2014a, 2017; Romans et al., 2016; Acharya and Chakrabarti, 2019; Liu et al., 2019).

A great number of studies have focused on sediments and their source-to-sink processes on many continental shelves in the world, such as the Sunda shelf in Southeast Asia (Hanebuth et al., 2000; Hanebuth and Statteger, 2004), the North Icelandic shelf (Eiriksson et al., 2000), and the ECS shelf in East Asia (Milliman et al., 1985a, 1985b; Li et al., 2005; Liu et al., 2006, 2007; Wang et al., 2013). Shelf sediment source-to-sink processes indicate great diversity in different sedimentary environments (Li et al., 2014a; Liu et al., 2016), especially in river sediment

inputs and ocean dynamic conditions, e.g., high energy, low sediment inputs in west European shelf (Stride, 1982) and on the contrary, low energy, high inputs in the Gulf of Papua shelf (Harris et al., 1996; Howell et al., 2014). Differently, it is well known that rivers draining the subtropical-tropical regions (most in East and South Asia) supply the largest loads of sediment discharge to the oceans (Meade, 1996; Milliman and Farnsworth, 2011), such as the Yangtze River ( $0.48 \text{ bt y}^{-1}$ ), Irrawaddy River ( $0.26 \text{ bt y}^{-1}$ ) and Mekong River ( $0.11 \text{ bt y}^{-1}$ ) (Fig. 1A). The Taiwan Strait, located on the southern East China Sea shelf (Fig. 1B), provides a significant link between the ECS and the South China Sea (SCS) and accumulates abundant land-derived sediments from mainland China and Taiwan island (Liu et al., 2008a; Xu et al., 2009, 2012; Horng

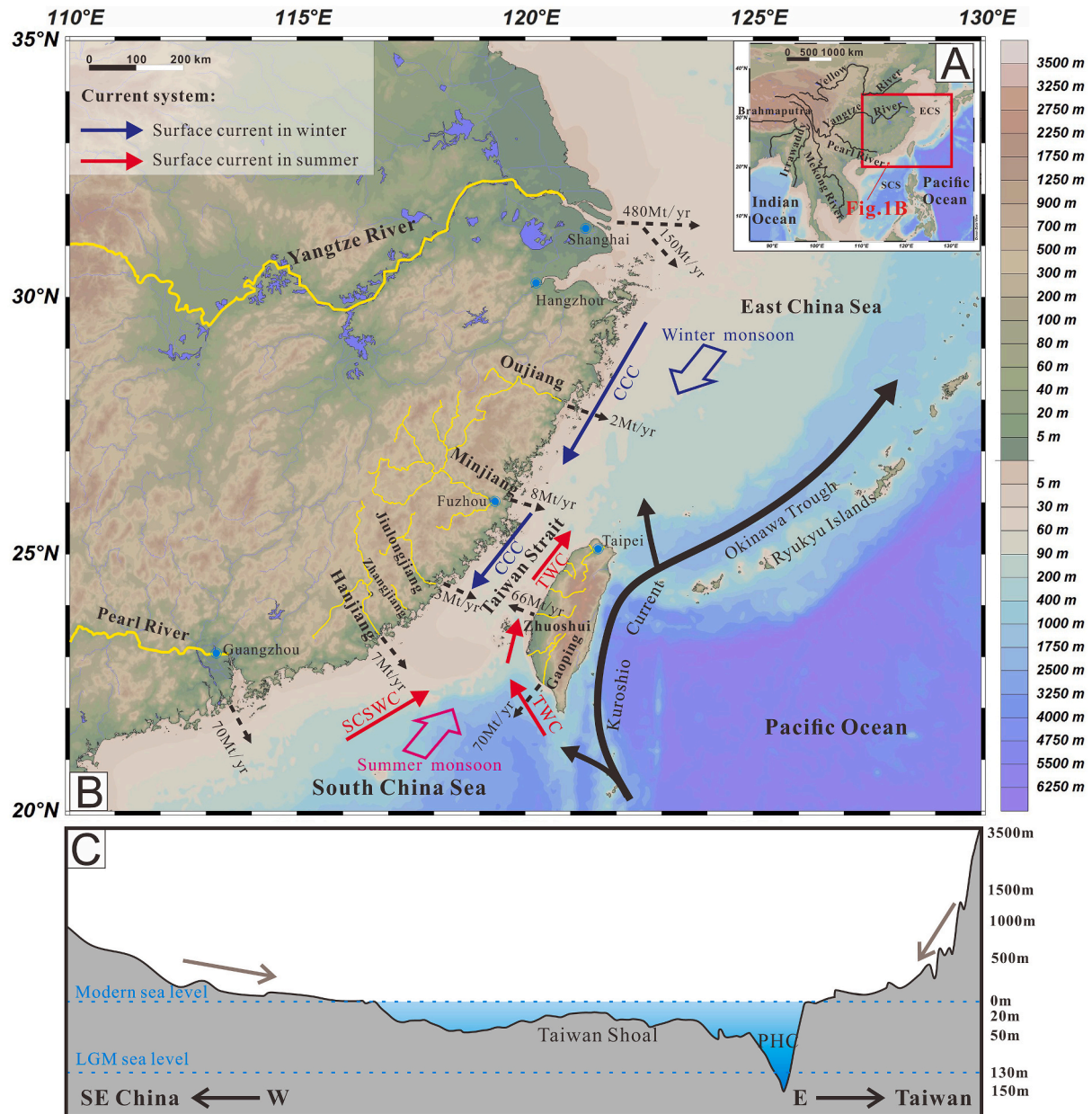


**Fig. 1.** (A) Location of the Taiwan Strait in the East Asia continental margin. Several large rivers are marked by black lines. (B) Major subtropical rivers in SE China and Taiwan, and their annual sediment discharge (data from Milliman and Meade, 1983; Meade, 1996; Xu et al., 2009). Dominated currents in Taiwan Strait and ECS and East Asian monsoon winds direction are marked. Red arrows represent warm currents, and blue arrows represent cold currents. CCC: China Coastal Current; SCSWC: South China Sea Warm Current; TWC: Taiwan Warm Current. (C) Schematic topography of a profile across Taiwan Shoal, Fujian Provenance and Taiwan western foothills. The shallowest part of Taiwan Shoal is up to 20 m, and Pengu Channel is deep to below 150 m. And a slow slope is showed in SE China side, whereas a rapid lift in the Taiwan side. LGM: Last glacial maximum. (For interpretation of the references to colour in this figure legend, the reader is referred to the web version of this article.)



and Huh, 2011; Huh et al., 2011). Furthermore, the Taiwan Strait is currently within an oceanic system with influences of both the ECS and SCS currents (wind-induced and tidal) and has a strong hydrodynamic condition (Wang et al., 2003). As a result, studies of sea floor sediments in the Taiwan Strait are useful to better understand sediment source-to-sink processes in a high sediment inputs and high energy sedimentary environment.

Previous studies show that the Taiwan Strait surficial sediments are dominated by sand in the south (Liu et al., 2008a) and muds in the north (Xu et al., 2009). During the past decades, a large number of studies have been made to document the history of the elongated inner-shelf mud belt, which extends 1000 km from the Yangtze River mouth to the northern Taiwan Strait (Liu et al., 2006, 2007, 2008a; Xu et al., 2009, 2012). According to high-resolution Chirp seismic profiles, Liu et al. (2006) documented the mud wedge which experienced different sediment accumulation rates in the past 11 kyr due to the East Asian monsoon climate, human activities and intensified currents (Xu et al., 2012). Detailed investigations on the inner-shelf mud wedge have been conducted and show that mud sediments in the northern Taiwan Strait are likely a product of Yangtze-derived clays driven by the China Coastal Current (CCC; Xu et al., 2009; Bi et al., 2015; Liu et al., 2018). However, sands in the southern Taiwan Strait remain poorly investigated. Adjacent rivers, such as the Minjiang, Hanjiang and Zhuoshui Rivers (Fig. 1B), provide approximately 100 million of tons of sediments into the Taiwan Strait annually, but these strait sands were previously regarded as relict sediment (Niino and Emery, 1961).

Early marine geologists divided the Taiwan Strait into three sedimentary regions (Qin, 1963). One outer shelf region which preserves coarse relict sands recycled from sedimentary strata deposited in the late Pleistocene low sea-level period, and two inner shelf regions, i.e., Zhejiang-Fujian coastal region and the Zhuoshui River mouth, which receive fine-grained modern river sediments. In last century 80–90s, published grain-size and heavy mineral data demonstrated that Taiwan

Strait sediments exhibited obvious spatial variations in composition. They proposed that relict sediments are mainly composed of coarse-medium sands and present in the Taiwan Shoal (Zeng et al., 1982; Chen, 1993). Besides, sediments on the Taiwan Shoal were also thought to be recycled sediments controlled by modern currents (Zheng and Zhang, 1982; Lan, 1991; Ma and Liu, 1994). Whether the Taiwan Strait sands are dominated by relict sediments remains to be proved and the fate of modern huge surrounding river-derived sand sediments remains poorly known.

In this study, the southern Taiwan Strait seafloor surficial sediments and adjacent river (Minjiang, Jiulongjiang, Zhangjiang, Hanjiang, Zhuoshui Rivers) riverbed sediments were collected (Fig. 2). The great differences of bedrock lithology between Southeastern (SE) China and the Taiwan island (Fig. 2) allow to track the Taiwan Strait sediment source-to-sink process by petrographic and heavy mineral analysis. The aims are to: (1) unravel the compositions and provenance of the Taiwan Strait surficial sands and (2) decipher controls on sediment spatial distributions in the Taiwan Strait.

## 2. Geological setting

The Taiwan Strait is located at the south of the ECS shelf, southwestward connecting with the SCS, bounded by the southeast coast of mainland China and Taiwan island to the west and east, respectively (Fig. 1B). The strait is about 350 km-long and 180 km-wide on average (140–200 km), with an average depth about 60 m. The bathymetry shows that Taiwan Strait is characterized by four distinctive topographic units (Fig. 2). The Changyun ridge (CYR) and the Taiwan Shoal are two shallow regions with average depths of ca. 20 m (Fig. 2). The former is located in the central-eastern Taiwan Strait and consists of eastern Changyun Sand Ridge, a sand shoal and a sand sheet (Liao et al., 2008), the latter is in the southwestern Taiwan Strait (Fig. 2). Two relatively deep-water units are the Penghu Channel and the Wuchu Depression.

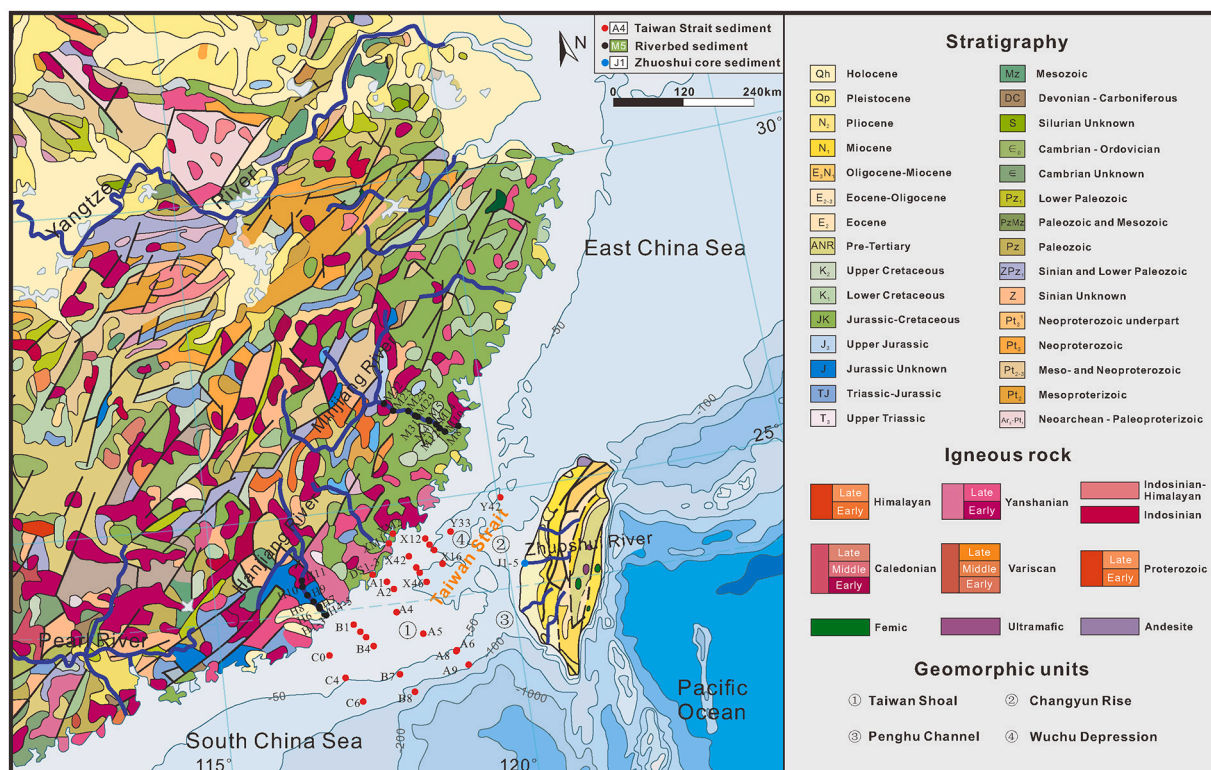


Fig. 2. Geological settings of the southeastern China (modified from Institute of Geology, Chinese Academy of Geological Sciences, 2002), with sampling locations (red dots: Taiwan Strait seafloor surficial sediment; black dots: riverbed sediment; blue dots: Zhuoshui River estuary down-core sediment). Submarine geomorphic units in the Taiwan Strait were marked. (For interpretation of the references to colour in this figure legend, the reader is referred to the web version of this article.)

These four submarine geomorphic units are proposed to comprise two conjugated tidal erosional and depositional systems (Liu et al., 1998), i. e., the Changyun ridge connects with the Penghu Channel in the east, and the Taiwan shoal couples with the Wuchu Depression in the west.

As mentioned above, the adjacent land regions around the strait spatially have significantly different geological and lithological backgrounds (Fig. 2). The Taiwan island is an accretionary orogen complex, composed of five tectonic units (Coastal Plain, Western Foothills, Xueshan Range, Central Range, Coastal Range), exposing Cenozoic sedimentary rocks and Mesozoic metamorphic rocks (Chang, 1975; Huang et al., 1997; Huang, 2017). The Taiwan island was initially exposed in an active subduction-collision region between the Eurasian continent and the Philippine Sea plate at 6.5 Ma (Huang et al., 2000, 2006). Now it is currently under a tectonically active background with frequent earthquakes (Dadson et al., 2004; Shyu et al., 2005; Huang, 2017). The Fujian Province, located on the Cathaysia block, consists of Precambrian basement metasedimentary rocks, Paleozoic sedimentary strata, and Jurassic-Cretaceous igneous rocks (Chen and Jahn, 1998; Li et al., 2014b; Jian et al., 2020a). The widespread Jurassic-Cretaceous igneous rocks are regarded as products of the westward subduction of the Paleo-Pacific Plate (Li et al., 2007, 2014b).

The East Asian monsoon serves as a major control on the current climatic conditions of the Taiwan Strait (Wang et al., 2000; Hu et al., 2012; Clift et al., 2014). Northeast wind and southwest wind prevail in winter and summer, respectively (Fig. 1). Under the control of monsoon climate, the ocean circulation in the Taiwan Strait displays seasonal variations. In winter, the CCC is intensified by the enhanced northeast wind. Southward flowing currents dominate in the Taiwan Strait and extend to the central Taiwan Strait (Fig. 1). During summer time, a branch of the Kuroshio current brings warm South China Sea water into the northern Taiwan Strait (Jan et al., 2002, 2006; Wu et al., 2007; Fig. 1). These ocean currents can move silt or clay sediments and thus control the distribution of surficial sediments (Xu et al., 2009; Liu et al., 2016). In addition, tides can also influence sediment distributions (Huang and Yu, 2003; Liao et al., 2008). The tides in Taiwan Strait are semidiurnal with a range of up to 4 m and average tidal current velocity is  $0.40 \text{ ms}^{-1}$  (Wang et al., 2003). As a result of large strong tidal currents, sand waves have formed in the tide-dominated shallow seas (Fig. 1 in Zhou et al., 2020). Frequent storm events with wave height higher than 10 m (including typhoons in summer and winter storms) play an important role in changing the sea floor morphology of shallow regions of the Taiwan Strait (Bao et al., 2020). It is wide accepted that sediment movement during storm events could change the morphometry of sand waves (Du et al., 2008; Bao et al., 2020; Zhou et al., 2020).

There are many mesoscale and small mountainous rivers on both sides of the Taiwan Strait, which are important transport pathways for land-derived sediments (Milliman and Syvitski, 1992; Yang et al., 2014b; Jian et al., 2020a, 2020b). Such rivers include the Minjiang, Jiulongjiang, Hanjiang Rivers on the west of the Taiwan Strait, and Zhuoshui, Kaoping Rivers on the east side (Fig. 1B). Due to background of drainage lithology, tectonics and climate, rivers on the two sides of the strait are largely different in sediment discharge and composition. On the one hand, each SE China river could deliver <10 Mt. of fluvial sediments per year, while the Zhuoshui River in Taiwan exports about 66 Mt. of sediments per year (Fig. 1B). On the other hand, the sediment transport and composition of mesoscale mountainous rivers in SE China, like the Minjiang River, are mainly controlled by hydroclimatic conditions (Jian et al., 2020b). However, the transport and composition of Taiwanese rivers-derived sediments are thought to be influenced by tectonic and climatic episodic events (Kao and Milliman, 2008; Liu et al., 2008a; Bi et al., 2015; Garzanti and Resentini, 2016).

### 3. Materials and methods

A total of 58 sediment samples covering the southern Taiwan Strait and adjacent exorheic rivers and estuaries were analyzed by

petrographic and heavy mineral analysis methods (sample locations are shown in Fig. 2). Twenty-six seafloor surficial sediment samples therein were collected in the southern Taiwan Strait by two cruises during 2016 and 2018. Twenty-seven samples were collected from the Minjiang, Jiulongjiang, Zhangjiang and Hanjiang Rivers in SE China. Lower reach samples are densely selected in the Minjiang and Hanjiang Rivers and estuaries sediments were collected in Jiulongjiang and Zhangjiang Rivers. Furthermore, five samples were collected from the Zhuoshui River mouth. More details are shown in Table A1 in Appendix A.

Bulk sample grain size distributions of 26 Taiwan Strait surficial sediments were analyzed by a Malvern laser particle analyzer (Master-sizer 3000) at Xiamen University. Samples were first treated by 10% HCl and 10%  $\text{H}_2\text{O}_2$  for chemically removing calcium carbonate ( $\text{CaCO}_3$ ) and organic matter, respectively. Then, 0.5 M ( $\text{NaPO}_3$ )<sub>4</sub> was added to avoid aggregation and 10 min ultrasonic treatment was conducted before the measurement.

In order to minimize the hydrodynamic sorting effect on the provenance analysis results, we focused on fine to medium sand components (0.063–0.5 mm). Each sample was wet-sieved and > 0.063 mm fractions were separated and dried. The 0.063–0.5 mm fractions of each sample obtained by dry sieving were used for framework petrography analysis (Ingersoll et al., 1984), and the 0.063–0.25 mm fractions were separated for transparent heavy mineral analysis. The 0.063–0.5 mm fractions of samples were saturated by Araldite and cut into standard thin sections. The Gazzi-Dickinson method was used to count the framework grains under a polarizing microscope (Dickinson and Suczek, 1979; Dickinson, 1985). The compositions (quartz, feldspar, lithic fragments) and textures of sediments were identified and documented. Heavy minerals were filtered by soaping in heavy liquid tribromomethane ( $2.89 \text{ g/cm}^3$ ), and subsequently fixed on glass slides by Canada balsam. Approximately 100 transparent heavy mineral grains were identified and counted under a polarizing microscope (Jian et al., 2020b).

Quantification of the quartz grain roundness was based on the criteria proposed by Wadell (1932). The definition of roundness is regarded as the ratio between the average of the radii of circles inscribed in corners and the radius of the maximum inscribed circle. A program by Resentini et al. (2018) was used to proceed binary image of quartz grains for each sample and obtain quantified results. According to the Wadell's criteria, grain roundness is divided into six grades: very angular = 0.12–0.17; angular = 0.17–0.25; subangular = 0.25–0.35; subrounded = 0.35–0.49; rounded = 0.49–0.70; well rounded = 0.7–1.0. To eliminate grain size effect on roundness, size of each analyzed grain was calculated using the equivalent spherical diameter (ESD; Garzanti et al., 2008). Grain length and width (X and Z) were measured directly from the thin sections under a polarizing microscope, and the third axis (Y) was estimated as equal to the measured width axis (Z). Then, the ESD of an ellipsoidal quartz grain is  $(X \cdot Y \cdot Z)^{1/3}$  (Lawrence et al., 2011).

## 4. Results

### 4.1. Bulk sample grain sizes

The grain size results of the Taiwan Strait sediments indicate that most analyzed samples (21 in 26) mainly consist of sand components with small amounts of silt and clay (Fig. A2 in Appendix B). Only two samples in the south of Taiwan Shoal and three samples in the central-western Taiwan Strait are dominated by silt components (ranging from 50% to 71%; Table A1 in Appendix A). Furthermore, sample A2 has 21% gravel-size components. Contents of fine to medium sands (the major targeted fraction in this study) vary from 8% to 100%. Except for five silt-dominated samples, fine to medium sand takes 64% in average in all sand components, with a minimum of 13% (sample A2) and a maximum of 100% (Fig. A2 in Appendix B). Spatially, medium-coarse sands are present in the Taiwan Shoal (with an average of 0.86  $\phi$ ) and its northwestern region (0.90  $\phi$  in average) and have a fining trend towards northern Taiwan Strait and south of Taiwan Shoal (Fig. 3A).



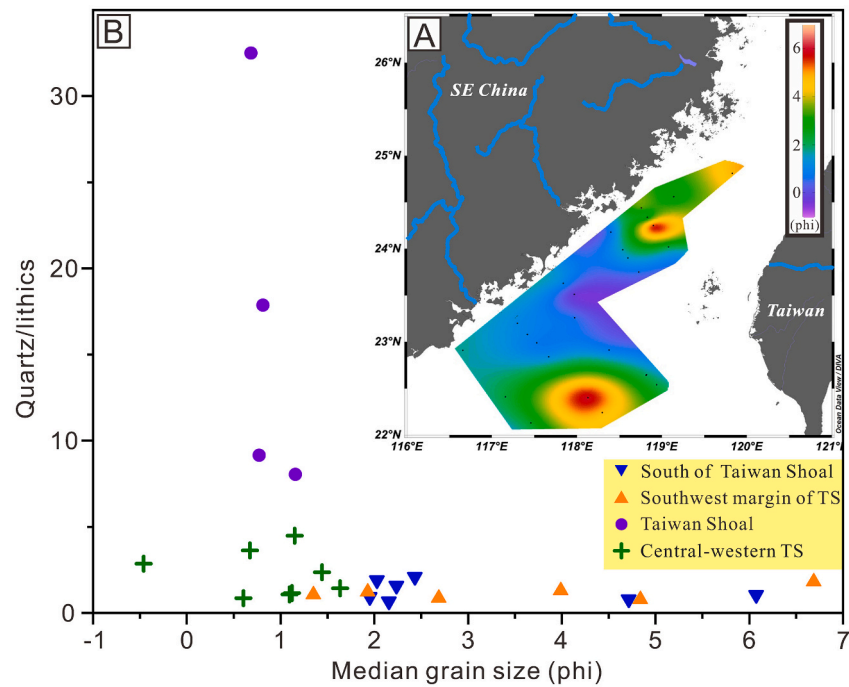


**Fig. 3.** Distribution of median grain size of bulk sediments in the surface Taiwan Strait (A), and its relationship with framework grain compositions (B). Except for Taiwan Shoal sediments with high contents of quartz, ratios between Quartz and Lithics has no increasing or decreasing tendency with median grain size.  $\phi$  ( $\phi$ ) =  $-\log_2(\text{diameter in mm})$ .

Median grain sizes of the central-western Taiwan Strait sediments are ranging from 1.35 to 6.73  $\phi$  (averaging 3.58  $\phi$ ) and that of the south of Taiwan Shoal is 3.08  $\phi$  (with maximum of 6.07  $\phi$ ).

#### 4.2. Framework grains

Sand samples collected from SE China rivers are moderately sorted

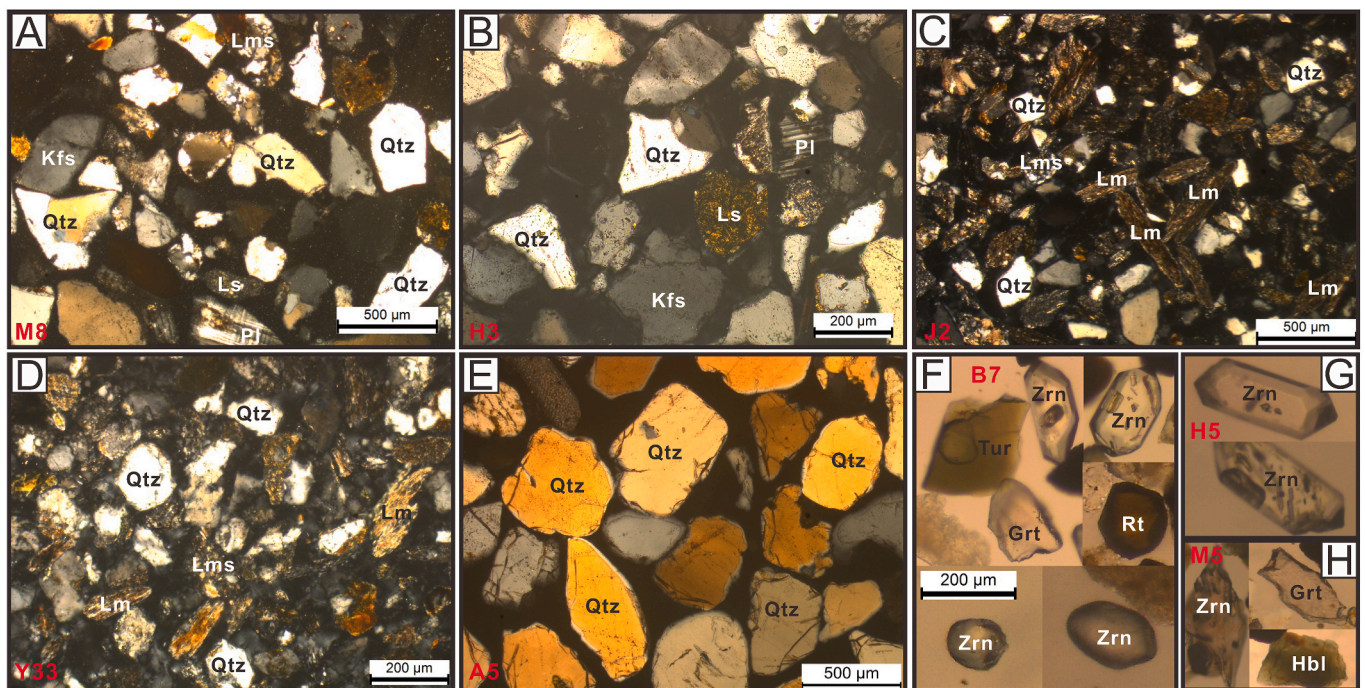


**Fig. 4.** Representative photomicrographs of sand samples. (A) and (B) dominated by slightly weathered quartz and feldspar (samples M8 and H3, Minjiang and Hanjiang Rivers, respectively). (C) low-rank metapelite fragments with a few quartz (sample J2, Zhuoshui River). (D) heavily weathered feldspar with low-rank metapelite fragments (samples Y33, central-western Taiwan Strait). (E) sub-rounded quartz (sample A5, Taiwan Shoal). (F) high ZTR index, and some zircons are well rounded (sample B7, south of Taiwan Shoal). (G) and (H) angular mineral particles collected in Hanjiang and Minjiang Rivers, respectively. Qtz: quartz; Kfs: K-feldspar; Pl: plagioclase; Ls: sedimentary rock fragments; Lms: metapelite fragments; Lm: metamorphic rock fragment; Zrn: zircon; Tur: tourmaline; Grt: garnet; Rt: rutile; Hbl: hornblende. Framework photos were taken under the cross-polarized light. Heavy minerals photos were taken under plane-polarized light.

and sub-angular (Fig. 4A–B; Fig. 5), while the Zhuoshui River sands are poorly sorted and sub-angular to rounded (Fig. 4C). The southern Taiwan Strait sands are featured by diverse textures and the grains are poorly-to-well sorted, and subangular to rounded (Fig. 5). The sands deposited in the southwest margin of Taiwan Strait and the central-western Taiwan Strait are subangular to subrounded and poorly sorted grains (Fig. 4D). Samples from the south of Taiwan Shoal are poorly sorted and subrounded, while samples from the Taiwan Shoal are well sorted and subrounded to rounded (Fig. 4E; Fig. 5).

The thin section point-counting data are plotted in the Q-F-L ternary diagram (Fig. 6A–B) and the raw data are shown in Table A1 in Appendix A. The SE China river-derived sands are dominated by quartz and feldspar, and the average content of quartz and feldspar reaches 86%. Sands of the Minjiang River are composed of 58% quartz, 31% feldspar and 11% lithic fragments (Fig. 7A). Similarly, the sands derived from the Hanjiang River comprise 67% quartz, (21%) feldspar and (8%) lithic fragments (Fig. 7A). However, the Zhuoshui River sands are dominated by lithic fragments (70%) with minor quartz and feldspar (Fig. 6A; Fig. 7A). The SE China river sands are relatively rich in volcanic lithic fragments (Fig. 6B), while the Zhuoshui River samples are rich in sedimentary and metasedimentary lithic fragments (Fig. 4C; Fig. 6C). Overall, sands in the southern Taiwan Strait display spatial compositional diversity, varying from feldspatho-quartzose to litho-quartzose sands (Fig. 6A; Fig. 7A). Sands deposited in southwest margin of Taiwan Strait are feldspatho-quartzose, with similar quartz and feldspar proportions to the composition of sand from SE rivers (Fig. 7A). The Taiwan Shoal sands are also feldspatho-quartzose, but have less lithic fragments than sands in the southwest margin of Taiwan Strait (Fig. 7A). Sands from the central-western Taiwan Strait and the south of Taiwan Shoal are mainly litho-quartzose and containing more lithic fragments (range from 19% to 55%) than other regions (Fig. 7A). Sedimentary lithic fragments are the major components of lithic grains in all the southern Taiwan Strait sand samples, while the contents of volcanic and metamorphic lithic fragments differ spatially (Fig. 6B).

#### 4.3. Heavy minerals

The transparent heavy mineral data are listed in Table A2 (Appendix A). Overall, heavy mineral assemblages vary from each river due to differences in drainage bedrock lithology (Fig. 6C). The Minjiang River sands ( $n = 10$ ) show high abundances of hornblende (18%) and garnet (17%), respectively. Stable heavy minerals, i.e., zircon, tourmaline and rutile (ZTR), account for 24% of heavy minerals, showing a relatively moderate mineralogical maturity. Besides, both epidote and pyroxene content exceed 10% (Fig. 7B). The heavy minerals in the Hanjiang River sands ( $n = 11$ ) are mainly consist of zircon (27%) and tourmaline (13%) with subordinate rutile (Fig. 7B). The high level of ZTR index values are represents high maturity of sediments compositions. However, heavy minerals in sands from the Zhuoshui River are dominated by garnet (average of 28%) and tourmaline, with partial chlorite and apatite (Fig. 7B). Heavy mineral assemblages are spatially diverse in the Taiwan Strait sands. Zircon is the major component for all samples, with an average content of 32% (maximum 61%), suggesting relatively high mineralogical maturity. Chlorite occupies the second place of abundance, ranging from 10% to 51%. Garnet, tourmaline, hornblende and monazite are the least abundant in heavy mineral assemblages (Fig. 7B).

#### 4.4. Quartz roundness

Roundness, which is a vital textural parameter of sand, reveals the textural maturity of sediments. The results of quartz roundness measurement are shown in Fig. 8 (details are in Table A3 in Appendix A). Overall, all the samples are dominated by subrounded (34%) to rounded (54%) quartz, with an average roundness of 0.46 to 0.62 (Fig. 8; Fig. A1 in Appendix B). Regionally, quartz grains in the Zhuoshui River have a higher average roundness (0.56) than the Minjiang (0.52) and Hanjiang (0.51) Rivers. Except for the inclusion of subrounded and rounded quartz, well rounded quartz grains are subordinate in the Zhuoshui River sands, whereas subangular quartz grains are minor components of sand in the Minjiang and Hanjiang Rivers (Fig. 8). Average roundness of

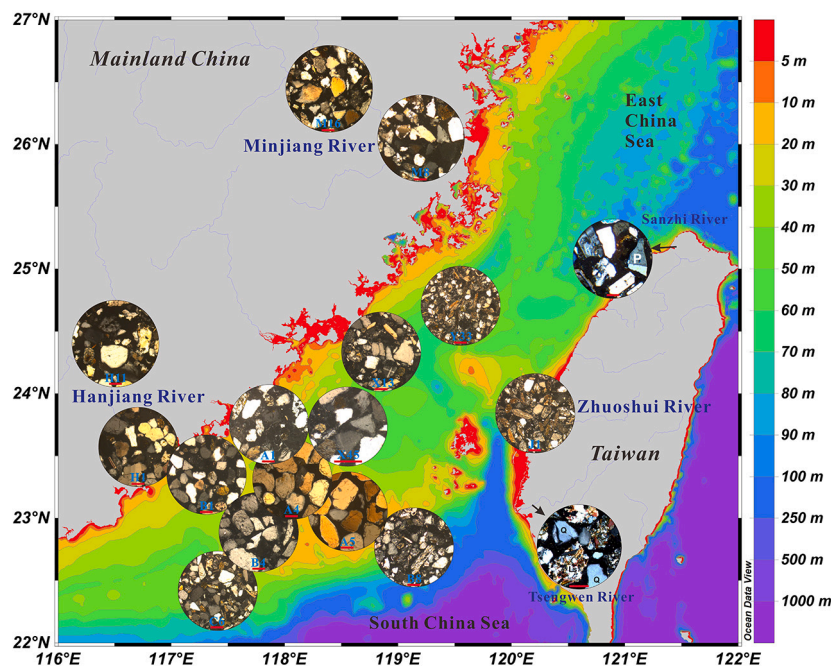


Fig. 5. Framework grains of Taiwan Strait surficial sands and adjacent rivers discharged sands. Compositional and textural differences between these sediments are explicit. Sanzhi River and Tsengwen River sediment photos are adapted from Garzanti and Resentini, 2016. All photos were taken under cross-polarized light; Red bar = 250  $\mu$ m. (For interpretation of the references to colour in this figure legend, the reader is referred to the web version of this article.)



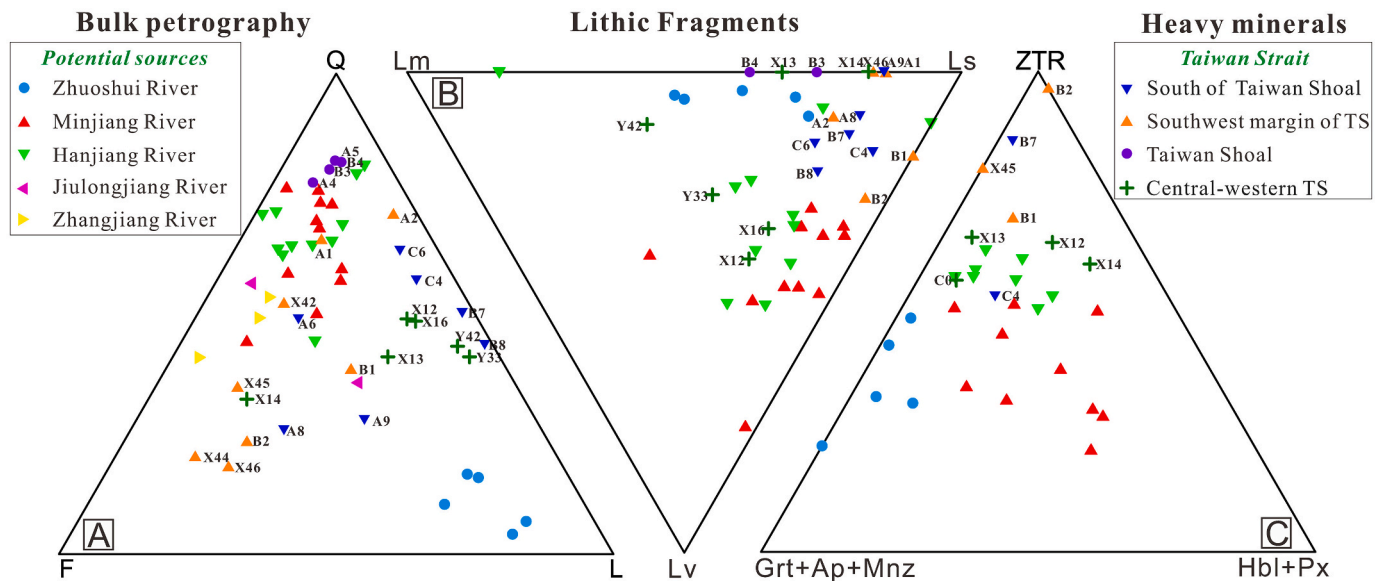


Fig. 6. Petrographic compositions of samples. QFL represents framework petrographic features, Lv-Ls-Lm illustrates source rocks' nature, heavy minerals reflex composition maturity and source rocks. Q: quartz; F: feldspar; L: lithic fragments; Ls: sedimentary rock fragments; Lv: volcanic rock fragments; Lm: metamorphic rock fragments; ZTR: zircon, tourmaline and rutile; Grt: garnet; Ap: apatite; Mnz: monazite; Hbl: hornblende; Px: pyroxene.

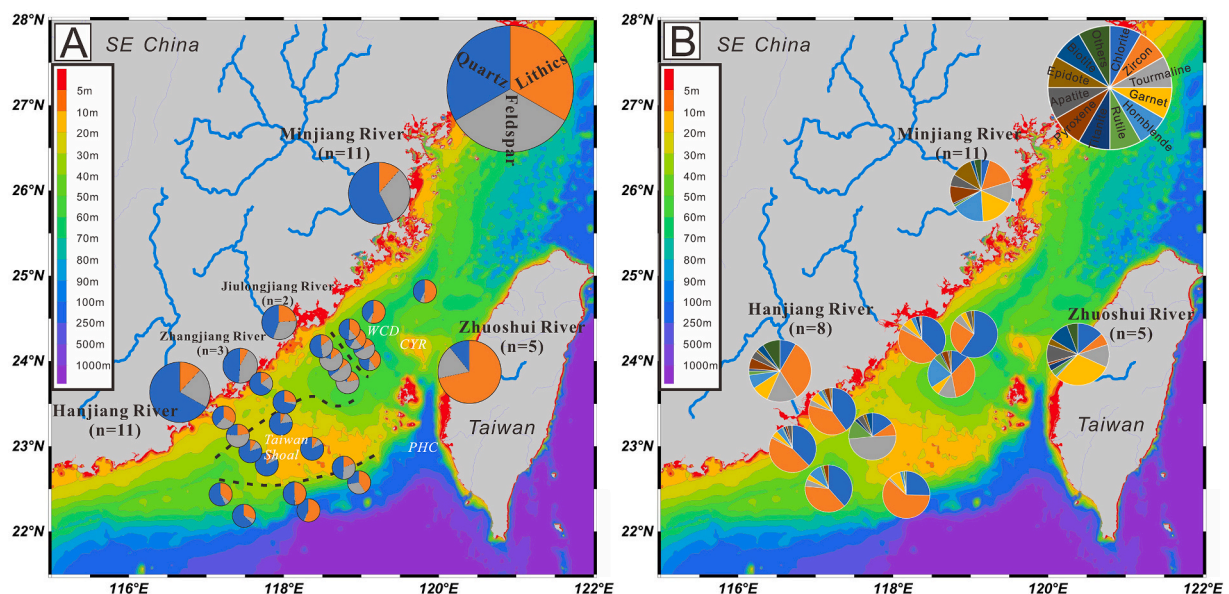


Fig. 7. Surface distribution of framework grain (A) and heavy mineral (B) compositions. Adjacent river samples are represented by average data (n is number of samples). High resolution submarine topography was shown and black dashed lines in (A) divide the Taiwan Strait into four sedimentary provinces based on compositions and submarine topography. CYR: Changyun Rise; PHC: Penghu Channel; WCD: Wuchu Depression.

quartz in the southern Taiwan Strait surficial sands ranges from 0.46 to 0.62. Specifically, the roundness of Taiwan Shoal quartz grains in the Taiwan Shoal have a narrow range with near 98% subrounded and rounded quartz (Fig. A1 in Appendix B). In contrast, quartz roundness in the other three regions vary widely, and quartz of other grades (i.e., very angular, angular, subangular and well rounded) comprises a higher fraction in southwest margin of Taiwan Strait (10%), central-western Taiwan Strait (14%) and south of Taiwan Shoal (10%).

## 5. Discussion

### 5.1. Provenance of the river sands

Our results demonstrate that sands from the SE China rivers are characterized by relatively high quartz and feldspar concentrations, high compositional maturity (Fig. 4A–B; Fig. 5; Fig. 6) and moderate textural maturity (Fig. 8). Sands from the Zhuoshui River in western Taiwan have abundant lithic fragments (sedimentary and low-rank metasedimentary lithic fragments) which are largely different from the SE China river sands (Fig. 5A; Fig. 7A). It is obvious that different bedrock lithologies of SE China and the Taiwan island are responsible for the distinct compositional signatures of the sediments discharged by



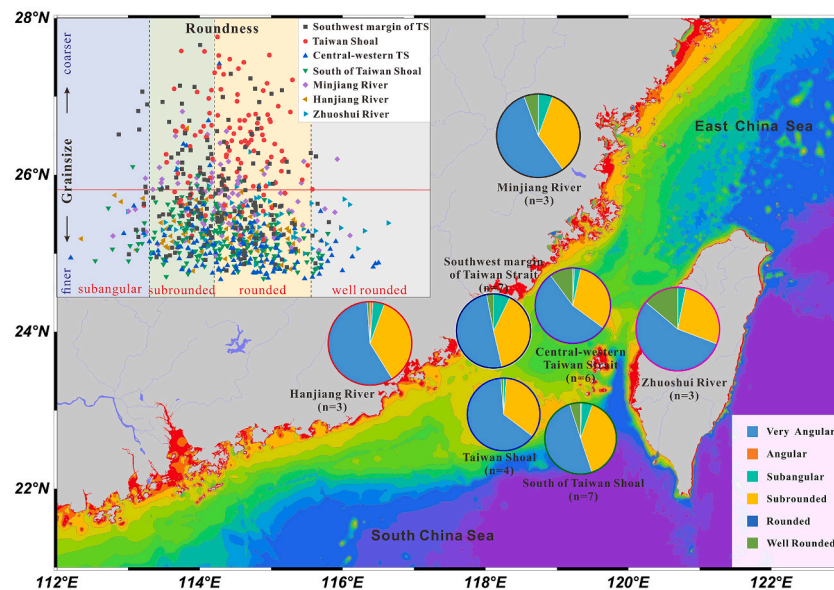


**Fig. 8.** All quartz grain roundness and composition of different grades of roundness in different sedimentary regions. The method of quantifying grain roundness follows with Wadell (1932), and computer processing method follows with Resentini et al., (2018).

those rivers.

For SE China, bedrock in the Minjiang and Hanjiang River catchments are mainly composed of Mesozoic granitoid rocks, Precambrian metamorphic rocks and subordinate Paleozoic sedimentary rocks (Chen and Jahn, 1998; Li et al., 2014b; Jian et al., 2020a; Fig. 2). And these rivers are under relatively stable tectonic settings, show relative long-term sediment transport (Li et al., 2016; Jian et al., 2020b) and thus tend to deliver compositionally mature sands into the ECS and the SCS. Specifically, Hanjiang River sands have more quartz contents and higher ZTR than those of the Minjiang River sands (Fig. 6). Increasing of rainfall intensity and corresponding weathering conditions make the Hanjiang River carry more contents of durable minerals (i.e., quartz and ZTR minerals) than the Minjiang River (He et al., 2020; Garzanti et al., 2021).

By contrast, bedrock in Taiwan is mainly composed of Cenozoic sedimentary and low-grade metasedimentary rocks (Chang, 1975; Huang et al., 1997; Huang, 2017; Fig. 2), resulting in high sedimentary and metasedimentary lithic fragment contents in sands discharged by the Zhuoshui River (Fig. 5; Fig. 6). Similar compositionally immature sediments can be found in other small mountainous rivers in Taiwan (Garzanti and Resentini, 2016; Fig. 5). The unique bedrock lithology and frequent extreme events (such as typhoon-triggered heavy rains and earthquake-induced landslides), rapid erosion, and relatively short transport distance jointly limit the maturity of Taiwanese river sands. Quartz grains in Zhuoshui River sands are featured by relative high quartz roundness (Fig. 8), which are likely due to sedimentary recycling (Garzanti and Resentini, 2016). These interpretations are also reinforced by the heavy mineral analysis results in this study (Fig. 6C; Fig. 7B).

## 5.2. Provenance of the southern Taiwan Strait sands and identification of depositional areas

Our results indicate that the southern Taiwan Strait sands have distinctive compositional and textural features. Based on sample locations and topography, in conjunction with the composition and texture of sand framework grain and heavy mineral assemblage, the Taiwan Strait can be divided into four sand depositional areas, i.e., 1) central-western Taiwan Strait; 2) southwest margin of Taiwan Strait; 3) Taiwan Shoal and 4) south of Taiwan Shoal (Fig. 7A).

The central-western Taiwan Strait includes eastward clinoform in the northwestern strait and north part of the Wuchu Depression, with Fujian Province (including Minjiang and Jiulongjiang Rivers) on the west side

and Changyun Rise on the east side (Fig. 7A). Water depth of six samples in this region ranges from 37 to 63 m. Framework grains consist of 42% quartz, 18% feldspar and 40% lithics fragments in average and thus represent as feldspatho-litho-quartzose sands. Note that lithic fragments in these samples, including sedimentary and metamorphic lithic fragments, take more proportions than in the SE China rivers sands (Fig. 7). Low-rank metasedimentary lithics fragments which dominate the Zhuoshui River sands are also found in this region (Fig. 5). This means that the lithic fragments in central-western Taiwan Strait sands can be sourced from Taiwan. The conclusion is consistent with previous magnetic property studies which demonstrate that sediments in the central-western Taiwan Strait have similar magnetic signals to the Taiwanese westward river sediments (Horn and Huh, 2011). In addition, seismic profiles in the northern Taiwan Strait, especially across the Changyun Rise, verify the progradation features around the Changyun Rise, indicating that the Changyun Rise could be a transport pathway for the central-western Taiwan Strait sands (Liao and Yu, 2005; Liu et al., 2008a). Liu et al. (2008a) conducted seismic profile investigations and down-core studies in the northern Taiwan Strait, and suggested that the Zhuoshui River predominantly supplied sediments to the Changyun Rise within the past 10 kyr. Furthermore, quartz and feldspar grains in central-western Taiwan Strait sands can be supplied by the SE China rivers.

The depositional area “southwest margin of the Taiwan Strait” locates on the northwest of the Taiwan Shoal near the south Fujian coast (Fig. 7A). The compositions of eight samples in this region are similar with the SE China river sands, which are feldspatho-quartzose or quartzo-feldspathic with low lithic fragment contents and are featured by high ZTR index values as well as moderate textural maturity (Fig. 6; Fig. 7). Thus, the southwest margin of Taiwan Strait is thought to be a major sink that received sands from the adjacent SE China rivers. Although the northern part of this area is close to the central-western Taiwan Strait through the Wuchu Depression, lithic contents are relatively low in samples from the southwest margin of Taiwan Strait which indicates few sands supply from the north.

The Taiwan Shoal is a salient submarine landform in the middle south Taiwan Strait with a total area of ~8800 km<sup>2</sup> and an average water depth of ~20 m (Liu et al., 1998; Fig. 7A). Four samples in this region are characterized by very high compositional maturity and moderate textural maturity. High contents of quartz indicate that sediments in the Taiwan Shoal are related to the SE China rivers. It is worth

noting that those quartz grains are coarse and rounded to well rounded (Fig. 5; Fig. 8) and are quite different with modern SE China rivers-derived sands. Therefore, modern rivers-derived sediments may not be the source of the Taiwan Shoal sands. Previous studies proposed that sands in the Taiwan Shoal were from the SE China paleo-rivers, but the sedimentary environments remain controversial (Niino and Emery, 1961; Zeng et al., 1982; Lan, 1991). Zeng et al. (1982) proposed that these sands were from detritus of fluvial or coastal facies exposing during the late Pleistocene low sea level period. On the contrary, based on grainsize and micropaleontology studies of surface and down-core sediments, medium-coarse sands in the Taiwan Shoal were thought to be carried by unidirectional currents from the Hanjiang River during 10 to 20 kyr B.P., and thus the Taiwan Shoal was in shallow sea environment (Lan, 1991; Cai et al., 1992). Therefore, the formation period and sediment transport around the Taiwan Shoal need further research.

The forth depositional area, south of Taiwan Shoal, is at the edge of the continental shelf and connects with SCS to the south (Fig. 7A). Submarine topography changes steeply in this region. Water depths of six samples in this region range from 40 to 190 m (Fig. 7A). Sand composition and texture in this region are similar with that of the central-western Taiwan Strait sands, indicating the co-contribution of SE China rivers and Taiwanese rivers (Fig. 6; Fig. 7). But this region is relatively far away from SE China and is separated by the Penghu Channel from Taiwan island. Therefore, how the terrestrial detritus was transported into this region remains an open question. Previous studies suggested that clay and silt sediments in the northern SCS were mainly from Taiwan by westward bottom currents (the westward branch of the North Pacific Deep Water and the Kuroshio Branch; Liu et al., 2008b; Cao et al., 2019). Although sand is much more difficult to be transported than clay/silt, the deep water might be the medium to carry the Taiwanese-river sediments to the south of the Taiwan Shoal. Besides, the Penghu Channel was thought to be formed by excavation of northward tidal currents since 15 kyr in the initial period of sea level rise (Huang and Yu, 2003; Liao and Yu, 2005). And paleo-rivers from SE China (e.g., paleo-Hanjiang, Jiulongjiang) and Taiwan might be potential sediment sources for the south of Taiwan Shoal before the formation of the channel.

Framework grain composition data are employed to model

contributions of the potential sources of the Taiwan Strait sands (Fig. 9). Specifically, the framework grain (quartz, feldspar and lithic fragment) compositions of the SE China river-sourced sands and Taiwan river-sourced sands are averaged and then serve as the two end-members (i. e., SE China and Taiwan) for the modeling (Fig. 9). Based on the average sand compositions of four regions, we estimate the sands of the central-western Taiwan Strait region are composed of 44% SE China-sourced and 56% Taiwan-sourced sands, while the south of Taiwan Shoal sands consist of 55% detritus from SE China and 45% detritus from Taiwan. Sands in another two regions, i.e., southwest margin of Taiwan Strait and Taiwan Shoal, are modeled to be dominated by SE China-sourced sands. However, sands from the Taiwan Shoal display higher  $(Q + F)/L$  values and have much higher textural maturity than the SE China river-sourced sands, indicating that these Taiwan Shoal sands experienced much stronger hydrodynamic alteration processes than the modern river sands.

### 5.3. Modern or relict sediments?

The concept of “Relict” sediment was first proposed by Emery (1952) and was applied to paleo-sediments that remain exposed on modern shelves after a rapid sedimentary environment change. Relict sediment usually refers to unreworked sediment type (Swift et al., 1971). It is well accepted that most of the modern continental shelves were exposed during the Last Glacial Maximum (LGM), when sea-level rose rapidly by about 130–140 m (Chappell, 1974; Fairbanks, 1989; Bard et al., 1990; Chappell and Polach, 1991; Mix et al., 2001). Rapid sea-level rise limited accommodation space on the continental shelves in some regions and relict sediments distribute widely on continental shelves over the world, for example, the North Sea floor, the Atlantic shelf, Northern Gulf of Mexico outer ECS shelf, etc. (Emery, 1968; Swift et al., 1971; Liu, 1990). Swift et al. (1971) reconsidered the relationship between “relict” sediments and local dynamic conditions, and then define the “palimpsest” sediment as “one exhibit petrographic attributes of an earlier depositional environment and, in addition, petrographic attributes of a later environment” (Swift et al., 1971, pp. 343). For example, sediments in the western Europe shelf with high energy and tidal-dominated regime, are extensively reworked producing a constructional seafloor topography and

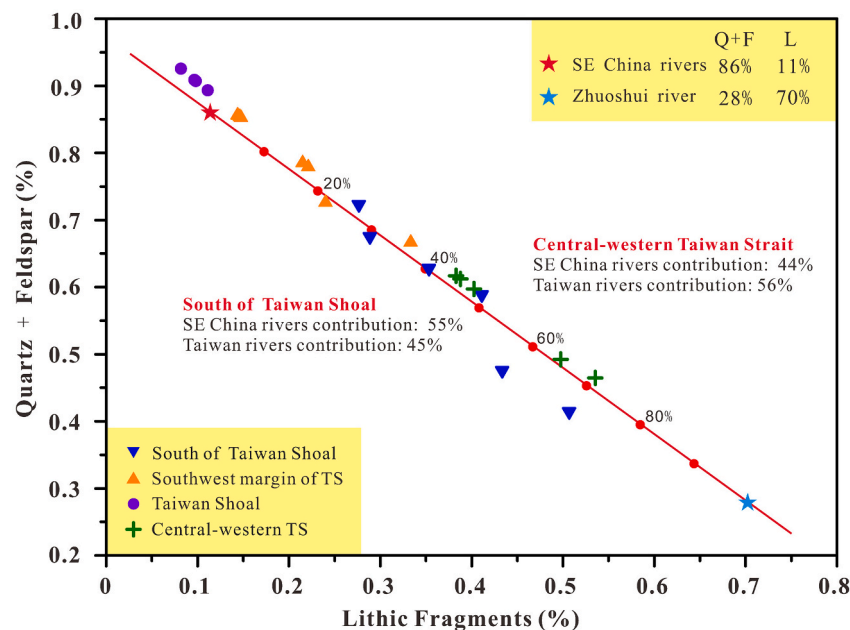


Fig. 9. Correlation of quartz + feldspar content with lithic fragments of sand samples. SE China rivers and Zhuoshui River are seen as two end-members, red line is mixing curve and divided into 10% increments (marked by red dots). Samples of our regions are plotted by different colors and shapes. (For interpretation of the references to colour in this figure legend, the reader is referred to the web version of this article.)

regional gradients (Swift et al., 1971). Relict sediments with obvious alternations by modern benthic organisms can also be regarded as palimpsest sediments (McManus, 1975).

Sediments in the Taiwan Strait and the outer ECS shelf (eastern Strait along Taiwan west shoreline) were regarded as relict sands in previous studies (Niino and Emery, 1961; Qin, 1963; Zeng et al., 1982; Liu, 1987; Li et al., 1991). In this study, the Taiwan Shoal is currently under a tidal-dominated regime with high energy. Sand petrographic features reflect that detritus materials were formed in an earlier depositional environment and have been reworked in oceanic environments. Besides, bulk analysis of sands in the Taiwan Shoal demonstrated high shell contents (Cai et al., 1992). Thus, although the Taiwan Shoal sands have little signal from modern river-derived sands (Fig. 5; Fig. 7), the modern sedimentary environment has indeed left traces on the sands of the Taiwan Shoal. With the Swift's definition in mind, sediments in the Taiwan Shoal might be better to be termed as palimpsest sediments.

Our new data indicate sands from Taiwan Shoal are medium to coarse with high compositional and textural maturity (Fig. 3; Fig. 7; Fig. 8). In-situ seafloor mapping results indicate that topography of the Taiwan Shoal is characterized by large sand waves which could be

observed in many tide-dominated shallow seas (Zhou et al., 2018). Heights of the sand waves range from 4.5 to 22.5 m and wavelengths cover a range from 244 to 2115 m (Zhou et al., 2020). More importantly, these sand waves could migrate due to wind-driven currents or tropical storm-induced waves (wave heights could exceed 10 m; Zhang et al., 2010; Campmans et al., 2017, 2018; Yu et al., 2017; Bao et al., 2020). Under the modern hydrodynamics conditions, the Taiwan Shoal surficial sediments are undergoing alternations by strong tidal and storm-induced wave currents, and therefore more stable minerals are expected to residue and tend to have high maturity. As a result, those relatively shallow regions in the Taiwan Strait might have high resource potentials for mineral placers (such as quartz and some stable heavy minerals).

For the other three depositional areas, composition and texture features are more similar with modern river-derived sands rather than sands in the Taiwan Shoal.  $^{210}\text{Pb}$ -based modern (<100 years) sedimentation rates estimation in the northern Taiwan Strait elucidated that Minjiang River sediments could be transported southward, but scarcely contribute to the central-western strait (Huh et al., 2011). Besides, sediments in the Taiwan Shoal might be a source for the southern shelf

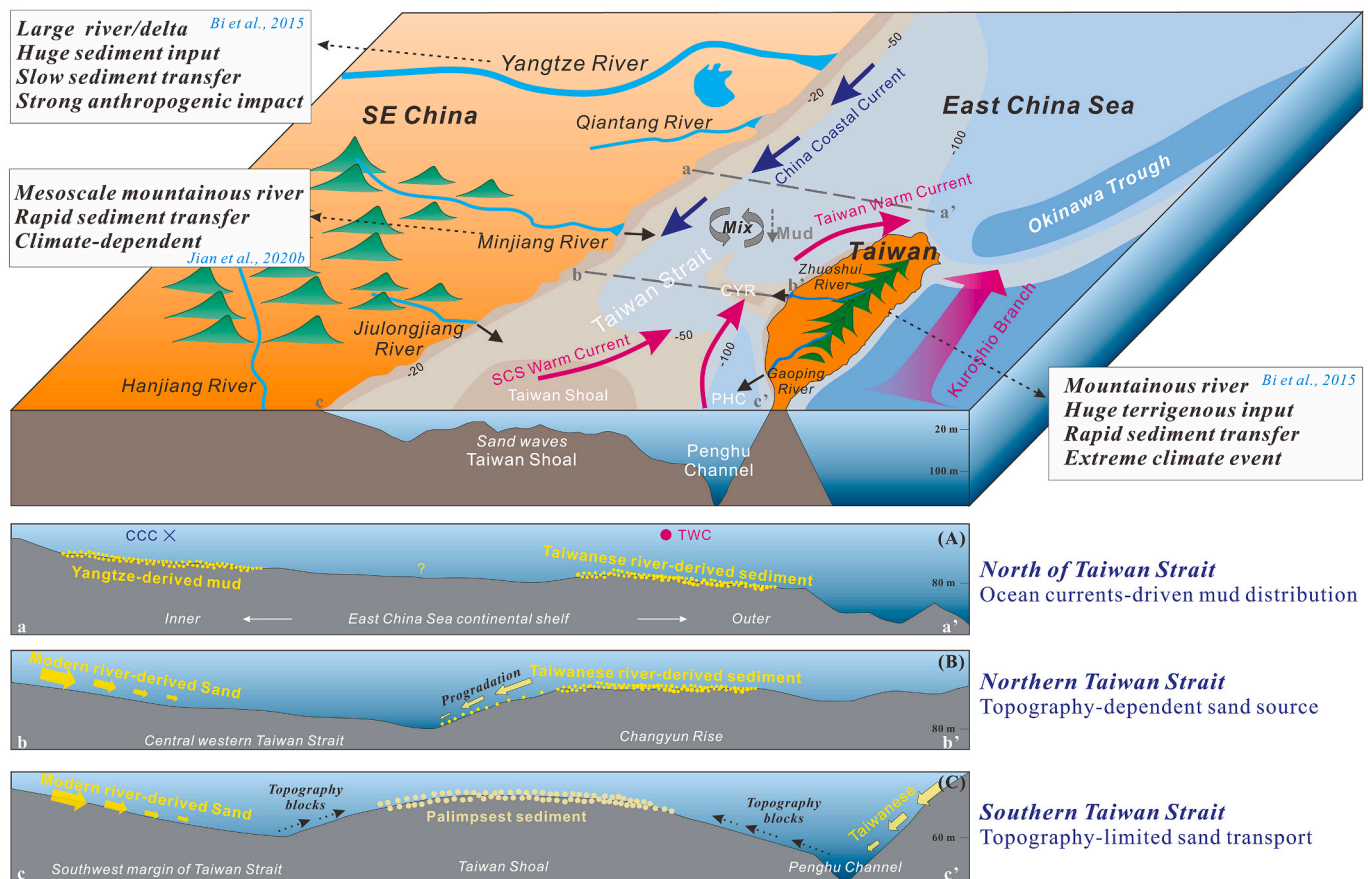


**Fig. 10.** Schematic sediment source-to-sink model around the East China Sea continental shelf and the Taiwan Strait. Simplified submarine topography was outlined. For sediment source, three distinct types of sediment supply and transport systems develop in subtropical-tropical East Asia (Bi et al., 2015; Jian et al., 2020b). Drainage basin bedrock lithology and morphology, tectonic settings, climatic conditions, and anthropogenic activities determine the differences in sediment flux and composition among these areas. Ocean currents and seafloor topography subsequently dominate the fate of river-derived sediment deposited on continental shelf. Three profiles cross the ECS shelf and the Taiwan Strait was marked with grey dashed lines. Profile (a) is at the south ECS shelf to the north of the Taiwan Strait. Yangtze River-derived clays carried by southward China Coastal Current (CCC) deposited along the Zhejiang-Fujian coast, and sediments derived by Taiwanese rivers are carried northward by Taiwan Warm Current and deposit near northern Taiwan island in outer ECS shelf. Profile (b) covers the Changyun Rise (water depth of 30 m) and the central-western Taiwan Strait. Due to high yield and episodic events, Taiwanese fluvial sediments on the Changyun Rise progressively prograde westward and form subaqueous delta (Liu et al., 2008a). Profile (c) indicates that topography contributes a major impact of sands distribution in the southern Taiwan Strait. The discharged sands of modern SE China rivers and Taiwanese rivers deposit in coastal region and are blocked by shallow submarine topography of the Taiwan Shoal. With less modern rivers-derived sediment, relict sediments are preserved in the Taiwan Shoal and experienced intensely alteration by high-energy hydrodynamic conditions.



margin, i.e., the south of Taiwan Shoal where water depth increases rapidly, through the southward migration of sand waves (Zhou et al., 2018) or gravity currents-induced collapse (Wang et al., 2020). Thus, relict or palimpsest sediments should also be considered to feed the three depositional areas, especially the regions close to the Taiwan Shoal. This means that the Taiwan Strait might also be a sediment source or a transport pathway for the surrounding deep ocean sediments, rather than a stable, constant sediment sink during the glacial-interglacial cycles. In this case, cautions should be exercised when studying sediment cores from the ECS, especially for determining depositional ages for core samples (e.g., possible depositional hiatus).

#### 5.4. Spatial variability of the submarine surficial sediments in the Taiwan Strait

As stated above, palimpsest (or relict) and modern sands co-exist in the Taiwan Strait and display spatially compositional and textural variability. The Taiwan Shoal, with average water depth of ca. 20 m, is covered by palimpsest sediments, whereas modern river-carried sediments are blocked by submarine topography and rarely contribute to the Taiwan Shoal (Fig. 10). Differently, the central-western Taiwan Strait and southwest margin surrounding the Taiwan Shoal with average water depths below 50 m could be sinks for the adjacent river-derived sediments (Fig. 10). The Changyun Rise, with water depth above 50 m could serve as a pathway for Taiwanese river-derived sediments to the central-western Taiwan Strait. The relatively steep slope in the south of Taiwan Shoal might result in sediment movements from the shallow Taiwan Shoal to this region. Therefore, we propose that submarine topography plays an important role in sand transport, distribution and composition in the Taiwan Strait. Furthermore, muds are widely distributed in the modern Taiwan Strait. Muds wedge along the Zhejiang-Fujian coast extending to the northern Taiwan Strait is one of the six distinct mud depocenters in the ECS (Liu et al., 2010; Xu et al., 2012; Li et al., 2014a). Numerous studies on seismic profiles, grain size and clay mineralogy involving both seafloor surface and down-core sediments have been made on the mud wedge along the inner shelf of the ECS (Liu et al., 2006, 2007, 2008a; Xu et al., 2009, 2012). Results show that Yangtze River-derived low-smectite and poor-illite crystallinity clays cover the inner ECS shelf and the northern Taiwan Strait, and Taiwanese river-derived clays only cover a narrow band in the Taiwan Strait (Xu et al., 2009). Most of these studies have highlighted a significant role of ocean currents in the mud sediment transport (Yang et al., 2003; Liu et al., 2004; Xiao et al., 2006; Xu et al., 2009, 2012; Xue et al., 2018; Fig. 10). Specifically, the China Coast Current enhanced by the East Asia winter monsoon transport Yangtze-derived muds to the Zhejiang-Fujian coastal and to the Taiwan Strait (Xu et al., 2009, 2012; Fig. 10). Collectively, we conclude that the Taiwan Strait surficial sediments are spatially composed of ocean current-dominated muds and submarine topography-related sands. These findings indicate the complexity of sediment source-to-sink processes around the Taiwan Strait and emphasize that sands and muds tend to have different fates in continental shelves with complex climate, ocean current and submarine topography conditions. Therefore, sediment grain sizes or specific size fractions should be clear when using sediment mineralogical and geochemical proxies to study source-to-sink processes in broad continental shelves.

## 6. Conclusions

In this study, we obtained framework grain and heavy mineral data from the southern Taiwan Strait seafloor surficial sands and adjacent river-sourced sediments to yield the following conclusions:

1. Southeastern China river sediments are rich in quartz and feldspar, whereas the western Taiwan mountainous river discharged sediments are dominated by sedimentary and low-rank metasedimentary

lithic fragments. This is consistent with bedrock geology of the river basins and indicates a bedrock lithology control on the composition of river sediment.

2. The investigated regions in the Taiwan Strait can be divided into four sedimentary provinces. The Taiwanese rivers contribute 56% and 45% sands to the central-western Taiwan Strait and the south of Taiwan Shoal, respectively, while the surficial sands in the southwest margin of Taiwan Strait are mainly provided by the SE China rivers. Sands from the Taiwan Shoal show extremely high compositional maturity and are mainly composed of coarse, rounded quartz. These highly mature sands, which were previously proposed as relict sediments, have been intensely altered by high-energy hydrodynamic conditions and thus are better to be termed as palimpsest sediments.
3. This study highlights a crucial role of submarine topography in the sand sediment distributions in broad and shallow continental shelves, which results in high spatially compositional and textural variability of the Taiwan Strait sands.

## Data availability

The data are available in the Appendix A and data archiving is also available at the Open Science Framework ([https://osf.io/dbh2j/?view\\_only=46e1183e952c4d5d9c0131f203ebe7f7](https://osf.io/dbh2j/?view_only=46e1183e952c4d5d9c0131f203ebe7f7)).

## Declaration of Competing Interest

The authors declare that they have no known competing financial interests or personal relationships that could have appeared to influence the work reported in this paper.

## Acknowledgments

This research was supported by the National Natural Science Foundation of China (Nos. 41806052, 41902126), Natural Science Foundation of Fujian Province (No. 2017J05067), Xiamen University Fundamental Research Funds for the Central Universities (Nos. 20720190097, 20720190103). Taiwan Strait sample collection was supported by the shared voyage of the National Natural Science Foundation. The funding for Zhuoshui River sample collection was provided by the ROC Ministry of Science and Technology under the grant numbers: NSC 99-2611-M110-005, NSC 100-2611-M-110-013 to J.T.L. We heartily thank Hanghai Liang and Dongming Hong for SE China river sediment sampling, and Zhichao Zhao for preparing Taiwan Strait samples. We are grateful to editor Edward Anthony and two anonymous reviewers for thorough and constructive comments on the manuscript.

## Appendix A. Supplementary data

Supplementary data to this article can be found online at <https://doi.org/10.1016/j.margeo.2021.106495>.

## References

- Acharya, S.S., Chakrabarti, R., 2019. Variations in trace metal concentrations and Sr, Nd isotopic compositions in sediments from two contrasting settings in the Eastern Arabian Shelf: implications for provenance and paleoclimate reconstruction. *Chem. Geol.* 509, 134–151. <https://doi.org/10.1016/j.chemgeo.2019.01.016>.
- Bao, J., Cai, F., Shi, F., Wu, C., Zheng, Y., Lu, H., Sun, L., 2020. Morphodynamic response of sand waves in the Taiwan Shoal to a passing tropical storm. *Mar. Geol.* 426, 1–11. <https://doi.org/10.1016/j.margeo.2020.106196>.
- Bard, E., Hamelin, B., Fairbanks, R.G., Zindler, A., 1990. Calibration of the  $^{14}\text{C}$  timescale over the past 30,000 years using mass spectrometric U-Th ages from Barbados corals. *Nature* 345, 405–410.
- Bi, L., Yang, S., Li, C., Guo, Y., Wang, Q., Liu, J.T., Yin, P., 2015. Geochemistry of river-borne clays entering the East China Sea indicates two contrasting types of weathering and sediment transport processes. *Geochem. Geophys. Geosyst.* 16 (9), 3034–3052. <https://doi.org/10.1002/2015gc005867>.
- Bi, L., Yang, S., Zhao, Y., Wang, Z., Dou, Y., Li, C., Zheng, H., 2017. Provenance study of the Holocene sediments in the Changjiang (Yangtze River) estuary and inner shelf of

- the East China sea. *Quat. Int.* 441, 147–161. <https://doi.org/10.1016/j.quaint.2016.12.004>.
- Cai, A., Zhu, X., Li, Y., Cai, Y., 1992. Sedimentary environment in Taiwan Shoal. *Chin. J. Oceanol. Limnol.* 10 (4), 331–339. <https://doi.org/10.1080/0264041031000071029>.
- Campmans, G.H.P., Roos, P.C., De Vriend, H.J., Hulscher, S.J.M.H., 2017. Modeling the influence of storms on sand wave formation: A linear stability approach. *Cont. Shelf Res.* 137, 103–116. <https://doi.org/10.1016/j.csr.2017.02.002>.
- Campmans, G.H.P., Ross, P.C., Vriend, H.J., Hulscher, S.J.M.H., 2018. The influence of storms on sand wave evolution: a nonlinear idealized modeling approach. *J. Geophys. Res. Earth Surf.* 123 (9), 2070–2086. <https://doi.org/10.1029/2018jfo04616>.
- Cao, L., Liu, J., Shi, X., He, W., Chen, Z., 2019. Source-to-sink processes of fluvial sediments in the northern South China Sea: constraints from river sediments in the coastal region of South China. *J. Asian Earth Sci.* 185 (104020) <https://doi.org/10.1016/j.jseas.2019.104020>.
- Chang, L., 1975. Biostratigraphy of Taiwan. *Geol. Paleontol. Southeast Asia* 15, 337–361.
- Chappell, J., 1974. Geology of coral terraces, Huon Peninsula, New Guinea: a study of quaternary tectonic movements and Sea-level changes. *Geol. Soc. Am. Bull.* 85 (4), 553–570.
- Chappell, J., Polach, H., 1991. Post-glacial sea-level rise from a coral record at Huon Peninsula, Papua New Guinea. *Nature* 349 (6305), 147–149.
- Chen, H., 1993. Characteristics and sources of heavy minerals in surface sediment of Taiwan Strait. *J. Oceanog. Taiwan Strait* 12, 136–144.
- Chen, J., Jahn, B.M., 1998. Crustal evolution of southeastern China: Nd and Sr isotopic evidence. *Tectonophysics* 284 (1–2), 101–133. [https://doi.org/10.1016/S0040-1951\(97\)00186-8](https://doi.org/10.1016/S0040-1951(97)00186-8).
- Clift, P.D., Wan, S., Blusztajn, J., 2014. Reconstructing chemical weathering, physical erosion and monsoon intensity since 25Ma in the northern South China Sea: A review of competing proxies. *Earth Sci. Rev.* 130, 86–102. <https://doi.org/10.1016/j.earscirev.2014.01.002>.
- Dadson, S.J., Hovius, N., Chen, H., Dade, W.B., Lin, J., Hsu, M., Lin, C., Horng, M., Chen, T., Milliman, J., Stark, C.P., 2004. Earthquake-triggered increase in sediment delivery from an active mountain belt. *Geology* 32 (8), 733–736. <https://doi.org/10.1130/g20639.1>.
- Deng, K., Yang, S., Li, C., Su, N., Bi, L., Chang, Y.P., Chang, S.C., 2017. Detrital zircon geochronology of river sands from Taiwan: Implications for sedimentary provenance of Taiwan and its source link with the east China mainland. *Earth Sci. Rev.* 164, 31–47. <https://doi.org/10.1016/j.earscirev.2016.10.015>.
- Deng, K., Yang, S., Bi, L., Chang, Y.P., Su, N., Frings, P., Xie, X., 2019. Small dynamic mountainous rivers in Taiwan exhibit large sedimentary geochemical and provenance heterogeneity over multi-spatial scales. *Earth Planet. Sci. Lett.* 505, 96–109. <https://doi.org/10.1016/j.epsl.2018.10.012>.
- Dickinson, W.R., 1985. Interpreting provenance relations from detrital modes of sandstones. In: Zuffa, G.G. (Ed.), *Provenance of Arenites*, pp. 333–361.
- Dickinson, W.R., Suczek, C.A., 1979. Plate tectonics and sandstone compositions. *Am. Assoc. Pet. Geol. Bull.* 63 (12), 2164–2182. <https://doi.org/10.1306/2F9188FB-16CE-11D7-8645000102C1865D>.
- Du, X., Li, Y., Gao, S., 2008. Characteristics of the large-scale sandwaves, tidal flow structure and bedload transport over the Taiwan Bank in southern China. *Acta Oceanol. Sin.* 30, 124–136.
- Eiriksson, J., Knudsen, K.L., Hafliðason, H., Henriksen, P., 2000. Late-glacial and Holocene palaeoceanography of the North Icelandic shelf. *J. Quat. Sci.* 15 (1), 23–42. [https://doi.org/10.1002/\(SICI\)1099-1417\(200001\)15:1<23::AID-JQS476>3.0.CO;2-8](https://doi.org/10.1002/(SICI)1099-1417(200001)15:1<23::AID-JQS476>3.0.CO;2-8).
- Emery, K.O., 1952. Continental shelf sediments off southern California. *Geol. Soc. Am. Bull.* 63, 1105–1108.
- Emery, K.O., 1968. Relict sediments on continental shelves of world. *Am. Assoc. Petrol. Geol. Bull.* 52 (3), 445–464.
- Fairbanks, R.G., 1989. A 17,000-year Glacio-Eustatic Sea-level record - influence of glacial melting rates on the younger dryas event and deep-ocean circulation. *Nature* 342 (6250), 637–642. <https://doi.org/10.1038/342637a0>.
- Garzanti, E., Resentini, A., 2016. Provenance control on chemical indices of weathering (Taiwan river sands). *Sediment. Geol.* 336, 81–95. <https://doi.org/10.1016/j.sedgeo.2015.06.013>.
- Garzanti, E., Andò, S., Vezzoli, G., 2008. Settling equivalence of detrital minerals and grain-size dependence of sediment composition. *Earth Planet. Sci. Lett.* 273 (273), 138–151. <https://doi.org/10.1016/j.epsl.2008.06.020>.
- Garzanti, E., He, J., Barbarano, M., Resentini, A., Li, C., Yang, L., Yang, S., Wang, H., 2021. Provenance versus weathering control on sediment composition in tropical monsoonal climate (South China) – 2. Sand petrology and heavy minerals. *Chem. Geol.* 564 (119997) <https://doi.org/10.1016/j.chemgeo.2020.119997>.
- Hanebuth, T.J.J., Statterger, K., 2004. Depositional sequences on a late Pleistocene–Holocene tropical siliciclastic shelf (Sunda Shelf, southeast Asia). *J. Asian Earth Sci.* 23 (1), 113–126. [https://doi.org/10.1016/s1367-9120\(03\)00100-7](https://doi.org/10.1016/s1367-9120(03)00100-7).
- Hanebuth, T.J.J., Statterger, K., Grootes, P.M., 2000. Rapid flooding of the sunda shelf: a late-glacial sea-level record. *Science* 288 (5468), 1033–1035. <https://doi.org/10.1126/science.288.5468.1033>.
- Harris, P.T., Pattiaratchi, C.B., Keene, J.B., Dalrymple, R.W., Gardner, J.V., Baker, E.K., Cole, A.R., Mitchell, D., Gibbs, P., Schroeder, W.W., 1996. Late Quaternary deltaic and carbonate sedimentation in the Gulf of Papua foreland basin: response to sea-level change. *J. Sediment. Res.* 66 (4), 801–819. <https://doi.org/10.1306/D426840F-2B26-11D7-8648000102C1865D>.
- He, J., Garzanti, E., Dinis, P., Yang, S., Wang, H., 2020. Provenance versus weathering control on sediment composition in tropical monsoonal climate (South China) - 1. Geochemistry and clay mineralogy. *Chem. Geol.* 558, 119860. <https://doi.org/10.1016/j.chemgeo.2020.119860>.
- Horng, C.S., Huh, C.-A., 2011. Magnetic properties as tracers for source-to-sink dispersal of sediments: A case study in the Taiwan Strait. *Earth Planet. Sci. Lett.* 309 (1–2), 141–152. <https://doi.org/10.1016/j.epsl.2011.07.002>.
- Howell, A.L., Bentley, S.S.J., Xu, K., Ferrell, J.R.E., Muhammad, Z., Septama, E., 2014. Fine sediment mineralogy as a tracer of latest Quaternary sediment delivery to a dynamic continental margin: Pandora Trough, Gulf of Papua, Papua New Guinea. *Mar. Geol.* 357, 108–122. <https://doi.org/10.1016/j.margeo.2014.08.003>.
- Hu, D., Böning, P., Köhler, C.M., Hillier, S., Pressling, N., Wan, S., Brumsack, H.J., Clift, P.D., 2012. Deep sea records of the continental weathering and erosion response to East Asian monsoon intensification since 14ka in the South China Sea. *Chem. Geol.* 326–327, 1–18. <https://doi.org/10.1016/j.chemgeo.2012.07.024>.
- Huang, C.Y., 2017. Geological ages of Taiwan stratigraphy and tectonic events. *Sci. Sin. Terrae* 47 (4), 394–405. <https://doi.org/10.1360/n072017-00023>.
- Huang, C.Y., Wu, W., Chang, C., Tsao, S., Yuan, P.B., Lin, C.W., Xia, K.Y., 1997. Tectonic evolution of accretionary prism in the arc-continent collision terrane of Taiwan. *Tectonophysics* 281 (1–2), 31–51. [https://doi.org/10.1016/S0040-1951\(97\)00157-1](https://doi.org/10.1016/S0040-1951(97)00157-1).
- Huang, C.Y., Yuan, P., Lin, C., Wang, T., Chang, C., 2000. Geodynamic processes of Taiwan arc-continent collision and comparison with analogs in Timor, Papua New Guinea, Urals and Corsica. *Tectonophysics* 325, 1–21. [https://doi.org/10.1016/S0040-1951\(00\)00128-1](https://doi.org/10.1016/S0040-1951(00)00128-1).
- Huang, C.Y., Yuan, P., Tsao, S., 2006. Temporal and spatial records of active arc-continent collision in Taiwan: A synthesis. *Geol. Soc. Am. Bull.* 118 (3–4), 274–288. <https://doi.org/10.1130/b25527.1>.
- Huang, Z., Yu, H., 2003. Morphology and geologic implications of Penghu Channel off southwest Taiwan. *Terr. Atmos. Ocean. Sci.* 14 (4), 469–485. [https://doi.org/10.3319/Tao.2003.14.4.469\(O\)](https://doi.org/10.3319/Tao.2003.14.4.469(O)).
- Huh, C.-A., Chen, W., Hsu, F., Su, C.C., Chiu, J.K., Lin, S., Liu, C.S., Huang, B.J., 2011. Modern (<100 years) sedimentation in the Taiwan Strait: Rates and source-to-sink pathways elucidated from radionuclides and particle size distribution. *Cont. Shelf Res.* 31 (1), 47–63. <https://doi.org/10.1016/j.csr.2010.11.002>.
- Ingersoll, R.V., Bullard, T.F., Ford, R.L., Grimm, J.D., Pickle, J.D., Sares, S.W., 1984. The effect of grain-size on detrital modes: a test of the Gazzi-Dickinson point-counting method. *J. Sediment. Petrol.* 54 (1), 103–116. <https://doi.org/10.1306/212F83B9-2B24-11D7-8648000102C1865D>.
- Institute of Geology, Chinese Academy of Geological Sciences, 2002. *Geological Atlas of China*.
- Jan, S., Wang, J., Chern, C., Chao, S., 2002. Seasonal variation of the circulation in the Taiwan Strait. *J. Mar. Syst.* 35 (3–4), 249–268. [https://doi.org/10.1016/S0924-7963\(02\)00130-6](https://doi.org/10.1016/S0924-7963(02)00130-6).
- Jan, S., Sheu, D.D., Kuo, H.M., 2006. Water mass and throughflow transport variability in the Taiwan Strait. *J. Geophys. Res.* 111 (C12) <https://doi.org/10.1029/2006jc003656>.
- Jian, X., Yang, S., Hong, D., Liang, H., Zhang, S., Fu, H., Zhang, W., 2020a. Seasonal geochemical heterogeneity of sediments from a subtropical mountainous river in SE China. *Mar. Geol.* 422, 1–13. <https://doi.org/10.1016/j.margeo.2020.106120>.
- Jian, X., Zhang, W., Yang, S., Kao, S.J., 2020b. Climate-dependent sediment composition and transport of Mountainous Rivers in Tectonically Stable, Subtropical East Asia. *Geophys. Res. Lett.* 47 (3), 1–11. <https://doi.org/10.1029/2019gl086150>.
- Kao, S.J., Milliman, J.D., 2008. Water and sediment discharge from small mountainous rivers, Taiwan: the roles of lithology, episodic events, and human activities. *J. Geol.* 116 (5), 431–448. <https://doi.org/10.1086/590921>.
- Lan, D., 1991. Preliminary study on age and origin of medium-coarse sands in Taiwan Shoal. *J. Oceanog. Taiwan Strait* 10, 156–161.
- Lawrence, R.L., Cox, R., Mapes, R.W., Coleman, D.S., 2011. Hydrodynamic fractionation of zircon age populations. *Grolog. Soc. Am. Bull.* 123 (1–2), 295–305. <https://doi.org/10.1130/b30151.1>.
- Li, C., Chen, G., Yao, M., Wang, P., 1991. The influences of suspended load on the sedimentation in the costal zones and continental shelves of China. *Mar. Geol.* 96, 341–352.
- Li, C., Yang, S., Zhao, J., Dosseto, A., Bi, L., Clark, T.R., 2016. The time scale of river sediment source-to-sink processes in East Asia. *Chem. Geol.* 446, 138–146. <https://doi.org/10.1016/j.chemgeo.2016.06.012>.
- Li, G., Liu, Y., Yang, Z., Yue, S., Yang, W., Han, X., 2005. Ancient Changjiang channel system in the East China Sea continental shelf during the last glaciation. *Sci. China Series D* 48 (11), 1972–1978. <https://doi.org/10.1360/04yd0053>.
- Li, G., Li, P., Liu, Y., Qiao, L., Ma, Y., Xu, J., Yang, Z., 2014b. Sedimentary system response to the global sea level change in the East China Seas since the last glacial maximum. *Earth Sci. Rev.* 139, 390–405. <https://doi.org/10.1016/j.earscirev.2014.09.007>.
- Li, X., Li, Z., Li, W., Liu, Y., Yuan, C., Wei, G., Qi, C., 2007. U–Pb zircon, geochemical and Sr–Nd–Hf isotopic constraints on age and origin of Jurassic I- and A-type granites from central Guangdong, SE China: A major igneous event in response to foundering of a subducted flat-slab? *Lithos* 96 (1–2), 186–204. <https://doi.org/10.1016/j.lithos.2006.09.018>.
- Li, Z., Qiu, J.S., Yang, X.M., 2014a. A review of the geochronology and geochemistry of Late Yanshanian (Cretaceous) plutons along the Fujian coastal area of southeastern China: implications for magma evolution related to slab break-off and rollback in the Cretaceous. *Earth Sci. Rev.* 128, 232–248. <https://doi.org/10.1016/j.earscirev.2013.09.007>.
- Liao, H.R., Yu, H.S., 2005. Morphology, hydrodynamics and sediment characteristics of the Changyung sand Ridge offshore Western Taiwan. *Terr. Atmos. Ocean. Sci.* 16 (3), 621–640. [https://doi.org/10.1016/0009-2614\(78\)80403-3](https://doi.org/10.1016/0009-2614(78)80403-3).

- Liao, H.R., Yu, H.S., Su, C.C., 2008. Morphology and sedimentation of sand bodies in the tidal shelf sea of eastern Taiwan Strait. *Mar. Geol.* 248 (3–4), 161–178. <https://doi.org/10.1016/j.margeo.2007.10.013>.
- Liu, F., Chang, X., Liao, Z., Yang, C., 2019. N-Alkanes as indicators of climate and vegetation variations since the last glacial period recorded in a sediment core from the northeastern South China Sea (SCS). *J. Asian Earth Sci.* 171, 134–143. <https://doi.org/10.1016/j.jseas.2018.09.018>.
- Liu, J., Saito, Y., Kong, X., Wang, H., Xiang, L., Wen, C., Nakashima, R., 2010. Sedimentary record of environmental evolution off the Yangtze River estuary, East China Sea, during the last 13,000 years, with special reference to the influence of the Yellow River on the Yangtze River delta during the last 600 years. *Quat. Sci. Rev.* 29, 2424–2438. <https://doi.org/10.1016/j.quascirev.2010.06.016>.
- Liu, J.P., Milliman, J.D., Gao, S., Cheng, P., 2004. Holocene development of the Yellow River's subaqueous delta, North Yellow Sea. *Mar. Geol.* 209 (14), 45–67. <https://doi.org/10.1016/j.margeo.2004.06.009>.
- Liu, J.P., Li, A., Xu, K., Velozzi, D.M., Yang, Z., Milliman, J.D., DeMaster, D.J., 2006. Sedimentary features of the Yangtze River-derived along-shelf clinoform deposit in the East China Sea. *Cont. Shelf Res.* 26 (17–18), 2141–2156. <https://doi.org/10.1016/j.csr.2006.07.013>.
- Liu, J.P., Xu, K., Li, A., Milliman, J.D., Velozzi, D.M., Xiao, S.B., Yang, Z.S., 2007. Flux and fate of Yangtze River sediment delivered to the East China Sea. *Geomorphology* 85 (3–4), 208–224. <https://doi.org/10.1016/j.geomorph.2006.03.023>.
- Liu, J.P., Liu, C., Xu, K., Milliman, J.D., Chiu, J.K., Kao, S.J., Lin, S., 2008a. Flux and fate of small mountainous rivers derived sediments into the Taiwan Strait. *Mar. Geol.* 256 (14), 65–76. <https://doi.org/10.1016/j.margeo.2008.09.007>.
- Liu, X., 1987. Relict sediments in China continental shelf. *Mar. Geol. Quat. Geol.* 7 (1), 1–14.
- Liu, X., 1990. Sedimentary districts of the Chinese continental shelf. *Mar. Geol. Quat. Geol.* 20, 13–22.
- Liu, X., Li, A., Dong, J., Lu, J., Huang, J., Wan, S., 2018. Provenance discrimination of sediments in the Zhejiang-Fujian mud belt, East China Sea: Implications for the development of the mud depocenter. *J. Asian Earth Sci.* 151, 1–15. <https://doi.org/10.1016/j.jseas.2017.10.017>.
- Liu, Z., Xia, D., Berne, S., Wang, K., Marsset, T., Tang, Y., Bourillet, J.F., 1998. Tidal deposition systems of China's continental shelf with special reference to the eastern Bohai Sea. *Mar. Geol.* 145, 225–253. [https://doi.org/10.1016/S0025-3227\(97\)00116-3](https://doi.org/10.1016/S0025-3227(97)00116-3).
- Liu, Z., Tuo, S., Colin, C., Liu, J.T., Huang, C.-Y., Selvaraj, K., Chen, C.-T.A., Zhao, Y., Siringan, F.P., Boulay, S., Chen, Z., 2008b. Detrital fine-grained sediment contribution from Taiwan to the northern South China Sea and its relation to regional ocean circulation. *Mar. Geol.* 255, 149–155. <https://doi.org/10.1016/j.margeo.2008.08.003>.
- Liu, Z., Zhao, Y., Colin, C., Stattegger, K., Wiesner, M.G., Huh, C.-A., Zhang, Y., Li, X., Sompochaiyaku, P., You, C., Huang, C., Liu, J.T., Siringan, F.P., Phon, L.K., Sathiamurthy, E., Hantoro, W.S., Liu, J., Tuo, S., Zhao, S., Zhou, S., He, Z., Wang, Y., Bunsomboonsakul, S., Li, Y., 2016. Source-to-sink transport processes of fluvial sediments in the South China Sea. *Earth Sci. Rev.* 153, 238–273. <https://doi.org/10.1016/j.earscirev.2015.08.005>.
- Ma, D., Liu, X., 1994. The formation and development of Taiwan Shoal. *Marine Geol. Lett.* 7, 4–6.
- McManus, D.A., 1975. Modern versus Relict sediment on the continental shelf. *Geol. Soc. Am. Bull.* 86, 1154–1160.
- Meade, R.H., 1996. River-sediment inputs to major delta. In: *Sea-Level Rise and Coastal Subsidence*, pp. 63–85.
- Milliman, J.D., Farnsworth, K.L., 2011. Runoff, erosion, and delivery to the Coastal Ocean. In: *River Discharge to the Coastal Ocean: a Global Synthesis*. Cambridge University Press, pp. 13–69. <https://doi.org/10.1017/CBO9780511781247.003>.
- Milliman, J.D., Meade, R.H., 1983. World-Wide delivery of river sediment to the oceans. *J. Geol.* 91 (1), 1–21. <https://doi.org/10.1086/628741>.
- Milliman, J.D., Syvitski, J.P.M., 1992. Geomorphic tectonic control of sediment discharge to the ocean - the importance of small mountainous rivers. *J. Geol.* 100 (5), 525–544. <https://doi.org/10.1086/629606>.
- Milliman, J.D., Beardsley, R.C., Yang, Z., Limeburner, R., 1985a. Modern Huanghe-derived muds on the Outer Shelf of the East China Sea—identification and potential transport mechanisms. *Cont. Shelf Res.* 4 (1–2), 175–188. [https://doi.org/10.1016/0278-4343\(85\)90028-7](https://doi.org/10.1016/0278-4343(85)90028-7).
- Milliman, J.D., Shen, H., Yang, Z., Meade, R.H., 1985b. Transport and deposition of river sediment in the changjiang estuary and adjacent continental-shelf. *Cont. Shelf Res.* 4 (1–2), 37–45. [https://doi.org/10.1016/0278-4343\(85\)90020-2](https://doi.org/10.1016/0278-4343(85)90020-2).
- Mix, A.C., Bard, E., Schneider, R., 2001. Environmental processes of the ice age: land, oceans, glaciers (EPILOG). *Quat. Sci. Rev.* 20 (4), 627–657. [https://doi.org/10.1016/S0277-3791\(00\)00145-1](https://doi.org/10.1016/S0277-3791(00)00145-1).
- Niino, H., Emery, K.O., 1961. Sediments of shallow portions of East China Sea and South China Sea. *Geol. Soc. Am. Bull.* 72, 731–762.
- Nittrouer, C.A., Demaster, D.J., 1986. Sedimentary processes on the Amazon continental-shelf - past, present and future-research. *Cont. Shelf Res.* 6 (1–2), 5–30. [https://doi.org/10.1016/0278-4343\(86\)90051-8](https://doi.org/10.1016/0278-4343(86)90051-8).
- Qin, Y., 1963. Primary study on topography and sediment type in the East China continental shelf seas. *Oceanologia et Limnologia Sinica* 5, 71–85.
- Rasmussen, T.L., Thomsen, E., Ślubowska, M.A., Jessen, S., Solheim, A., Koç, N., 2007. Paleocceanographic evolution of the SW Svalbard margin (76°N) since 20,000 14C yr BP. *Quat. Res.* 67 (1), 100–114. <https://doi.org/10.1016/j.yqres.2006.07.002>.
- Resentini, A., Andò, S., Garzanti, E., 2018. Quantifying roundness of detrital minerals by image analysis: sediment transport, shape effects, and provenance implications. *J. Sediment. Res.* 88 (2), 276–289. <https://doi.org/10.2110/jsr.2018.12>.
- Romans, B.W., Castellort, S., Covault, J.A., Fildani, A., Walsh, J.P., 2016. Environmental signal propagation in sedimentary systems across timescales. *Earth Sci. Rev.* 153, 7–29. <https://doi.org/10.1016/j.earscirev.2015.07.012>.
- Shyu, J.B.H., Sieh, Y.-G., Chen, Y.-G., Liu, C.-S., 2005. Neotectonic architecture of Taiwan and its implications for future large earthquakes. *J. Geophys. Res.* 110 (B8), 1–33. <https://doi.org/10.1029/2004jb003251>.
- Stride, A.H. (Ed.), 1982. *Offshore Tidal Sands - Processes and Deposits*. Chapman and Hall, London.
- Swift, D.J.P., Stanley, D.J., Curran, J.R., 1971. Relict sediments on continental shelves: a reconsideration. *J. Geol.* 79, 324–346.
- Thomas, H., Bozec, Y., Elkalay, K., De Baar, H.J.W., 2004. Enhanced open ocean storage of CO<sub>2</sub> from shelf sea pumping. *Science* 304 (5673), 1005–1008. <https://doi.org/10.1126/science.1095491>.
- Wadell, H., 1932. Volume, shape, and roundness of rock particles. *J. Geol.* 40, 443–451.
- Wang, B., Wu, R., Fu, X., 2000. Pacific–East Asian teleconnection: how does ENSO affect East Asian climate? *J. Clim.* 13, 1517–1536. [https://doi.org/10.1175/1520-0442\(2000\)013<1517:PEATHD>2.0.CO;2](https://doi.org/10.1175/1520-0442(2000)013<1517:PEATHD>2.0.CO;2).
- Wang, P., 1999. Response of Western Pacific marginal seas to glacial cycles: paleoceanographic and sedimentological features. *Mar. Geol.* 156, 5–39. [https://doi.org/10.1016/S0025-3227\(98\)00172-8](https://doi.org/10.1016/S0025-3227(98)00172-8).
- Wang, Y., Jan, S., Wang, D., 2003. Transports and tidal current estimates in the Taiwan Strait from shipboard ADCP observations (1999–2001). *Estuar. Coast. Shelf Sci.* 57 (1–2), 193–199. [https://doi.org/10.1016/S0272-7714\(02\)00344-X](https://doi.org/10.1016/S0272-7714(02)00344-X).
- Wang, Y., Wu, Z., Shang, J., Yin, S., Zhao, D., Zhou, J., 2020. Morphologic characteristics and controlling factors of the northeastern South China Sea canyon group. *Acta Oceanol. Sin.* 42 (11), 62–74.
- Wang, Z., Yang, S., Zhang, Z., Lan, X., Gu, Z., Zhang, X., 2013. Paleo-fluvial sedimentation on the outer shelf of the East China Sea during the last glacial maximum. *Chin. J. Oceanol. Limnol.* 31 (4), 886–894. <https://doi.org/10.1007/s00343-013-2253-5>.
- Wu, C.R., Chao, S.Y., Hsu, C., 2007. Transient, seasonal and interannual variability of the Taiwan Strait current. *J. Oceanogr.* 63 (5), 821–833. <https://doi.org/10.1007/s10872-007-0070-1>.
- Xiao, S., Li, A., Liu, J.P., Chen, M., Xie, Q., Jiang, F., Li, T., Xiang, R., Chen, Z., 2006. Coherence between solar activity and the East Asian winter monsoon variability in the past 8000 years from Yangtze River-derived mud in the East China Sea. *Paleogeogr. Palaeoclimatol. Palaeoecol.* 237 (2–4), 293–304. <https://doi.org/10.1016/j.palaeo.2005.12.003>.
- Xu, K., Milliman, J.D., Li, A., Liu, J.P., Kao, S.J., Wan, S., 2009. Yangtze- and Taiwan-derived sediments on the inner shelf of East China Sea. *Cont. Shelf Res.* 29 (18), 2240–2256. <https://doi.org/10.1016/j.csr.2009.08.017>.
- Xu, K., Li, A., Liu, J.P., Milliman, J.D., Yang, Z., Liu, C.S., Kao, S.J., Wan, S., Xu, F., 2012. Provenance, structure, and formation of the mud wedge along inner continental shelf of the East China Sea: A synthesis of the Yangtze dispersal system. *Mar. Geol.* 291–294, 176–191. <https://doi.org/10.1016/j.margeo.2011.06.003>.
- Xue, C., Qin, Y., Ye, S., Laws, E.A., Wang, Z., 2018. Evolution of Holocene ebb-tidal clinoform off the Shandong Peninsula on East China Sea shelf. *Earth Sci. Rev.* 177, 478–496. <https://doi.org/10.1016/j.earscirev.2017.12.012>.
- Yang, R.J., Liu, J.T., Fan, D., Burr, G.S., Lin, H.L., Chen, T.T., 2017. Land-sea duel in the late Quaternary at the mouth of a small river with high sediment yield. *J. Asian Earth Sci.* 143, 59–76. <https://doi.org/10.1016/j.jseas.2017.03.028>.
- Yang, S., Jung, H., Lim, D., Li, C., 2003. A review on the provenance discrimination of sediments in the Yellow Sea. *Earth Sci. Rev.* 63 (1–2), 93–120. <https://doi.org/10.1016/j.earscirev.2014.07.006>.
- Yang, S., Milliman, J.D., Xu, K., Deng, B., Zhang, X., Luo, X., 2014a. Downstream sedimentary and geomorphic impacts of the Three Gorges Dam on the Yangtze River. *Earth Sci. Rev.* 138, 469–486. [https://doi.org/10.1016/S0012-8252\(03\)00033-3](https://doi.org/10.1016/S0012-8252(03)00033-3).
- Yang, S., Wang, Z., Dou, Y., Shi, X., 2014b. Chapter 21 a review of sedimentation since the Last Glacial Maximum on the continental shelf of eastern China. *Geol. Soc. Lond. Mem.* 41 (1), 293–303. <https://doi.org/10.1144/m41.21>.
- Yu, X., Pan, W., Zheng, X., Zhou, S., Tao, X., 2017. Effects of wave-current interaction on storm surge in the Taiwan Strait: insights from Typhoon Morakot. *Cont. Shelf Res.* 146, 47–57. <https://doi.org/10.1016/j.csr.2017.08.009>.
- Zeng, C., Zhu, Y., Wang, X., 1982. Bottom material types and sedimentation districts in Taiwan Strait. *Taiwan Strait* 1, 54–61.
- Zhang, W., Shi, F., Hong, H., Shang, S., Kirby, J.T., 2010. Tide-surge Interaction Intensified by the Taiwan Strait. *J. Geophys. Res.* 115 (C6), 1–17. <https://doi.org/10.1029/2009jc005762>.
- Zheng, T., Zhang, J., 1982. A Preliminary Study on the Topography and Sedimentary Characteristics of Taiwan Bank and the Continental Shelf. *The Geology of the Yellow Sea and the East China Sea*, Science Press, Beijing, pp. 52–66.
- Zhou, J., Wu, Z., Jin, X., Zhao, D., Cao, Z., Guan, W., 2018. Observations and analysis of giant sand wave fields on the Taiwan Banks, northern South China Sea. *Mar. Geol.* 406, 132–141. <https://doi.org/10.1016/j.margeo.2018.09.015>.
- Zhou, J., Wu, Z., Zhao, D., Guan, W., Zhu, C., Flemming, B., 2020. Giant sand waves on the Taiwan Banks, southern Taiwan Strait: Distribution, morphometric relationships, and hydrologic influence factors in a tide-dominated environment. *Mar. Geol.* 427, 1–12. <https://doi.org/10.1016/j.margeo.2020.106238>.